Discovery and Analysis of a Major Lipid Droplet Protein in a Marine Diatom *Phaeodactylum tricornutum*

A Dissertation submitted to
the Graduate School of Life and Environmental Sciences,
the University of Tsukuba
in Partial Fulfillment of the Requirements
for the Degree of Doctor of Philosophy in Science
(Doctoral Program in Integrative Environmental Sciences)

Kohei YONEDA

Table of Contents

List of Tables

List of Figures

Abstract

Various kinds of organisms, including microalgae, accumulate neutral lipids in distinct intracellular compartments called lipid droplets. Generally, lipid droplets are generated from the endoplasmic reticulum and particular proteins localize on their surface. Some of these proteins function as structural proteins to prevent fusion between the lipid droplets, and the others could have an enzymatic role or might be involved in intracellular membrane trafficking. However, information about lipid droplet proteins in microalgae is scarce as compared with that in animals and land plants. I focused on the oil-producing, marine, pennate diatom *Phaeodactylum tricornutum* that forms lipid droplets during nitrogen deprivation and I investigated the proteins located on the lipid droplets. After 6 days of cultivation in a nitrate-deficient medium, the mature lipid droplets were isolated by sucrose density gradient centrifugation. Proteomic analyses revealed five proteins, with Stramenopile-type lipid droplet protein (StLDP) being the most abundant protein in the lipid droplet fraction. Though the primary sequence of StLDP did not have homology to any known lipid droplet proteins, StLDP had a central hydrophobic domain. This structural feature is also detected in oleosin of the land plant and lipid droplet surface protein (LDSP) of the *Nannochloropsis*. As a proline knot motif of oleosin, conservative proline residues existed in the hydrophobic domain. StLDP was upregulated during nitrate deprivation and fluctuations of StLDP expression levels corresponded with the size of the lipid droplets.

Then, I produced *P. tricornutum* mutant that expressed homologous StLDP gene under the control of fcpA promoter to deduce the function. Expression of StLDP was strongly enhanced especially when the mutant cultivated in nitrogen sufficient medium but the expression level attenuated in the nitrogen deficient medium. Despite the strong expression, lipid droplet formation was not observed and there was no significant different in lipid composition under nitrogen sufficient condition in both wild type (WT) and StLDP-expressing mutant (H8). After the cultivation in nitrogen deficient medium for 6 days, neutral lipid content significantly

increased and larger size of lipid droplet observed in H8 compared to WT. However, the total lipid yield did not increase in H8 mutant. At the 2-day in nitrogen deficiency, 97.0% of single cells in WT formed one or two lipid droplet(s), while the proportion of the cells that formed one or two lipid droplet(s) decreased to 78.8% in H8 mutant and the one that formed three or four lipid droplets increased (15.1% and 6.0%, respectively). It was suggested that StLDP facilitated sequestration of TAG at the initial stage of lipid droplet formation and it led to the increase of neutral lipid content in H8 mutant.

Key words:
Diatom, Lipid droplet protein, Triacylglycerol, Nitrogen deprivation, *Phaeodactylum tricornutum*, Proteomic analysis

General Introduction

Lipids are usually defined as hydrophobic and amphipathic molecules of biological origin that cannot be soluble in water but in organic solvents. They may be classified into eight categories in two distinct groups that based on the substrates (so-called “building blocks”) in the biosynthesis: fatty acyls, glycerolipids, glycerophospholipids, sphingolipids, saccharolipids, and polyketides (entirely or partially derived from condensations of thioesters); prenol lipids and sterol lipids (derived from condensations of isoprene units) (Fahy et al. 2009). One of the fundamental features of lipids is that they have higher calorific value per weight than carbohydrate. The calorific value of fat is ca. 9 kcal/g while that of carbohydrate is ca. 4 kcal/g. Neutral glycerolipids chiefly triacylglycrids (TAG), which have three fatty acid moieties bound to glycerol backbone, serve as carbon and energy depot in the eukaryotes. Multi-cellular organisms accumulate TAG-based energy storage in specific tissues such as mammalian adipose tissues and plant seeds. As well as storage lipids, they accumulate carbohydrate-based energy storage such as glycogen in liver tissue and starch in plastids. Calorific values per unit weight of such polysaccharides are lower than that of lipids, but the carbohydrates differ from the lipids in its hydrophilicity. Biochemical reaction *in vivo* should occur in aqueous fraction of the cell through the bio-catalytic proteins, so water solubility of the substances and the contact to the enzymes are important on the reaction. Sugar unit of these polysaccharides is typically water soluble, so it can easily react with the cytosolic enzymes. On the degradation of TAG, the first reaction is catalyzed by lipases that remove fatty acid moiety from the TAG. The lipases can only react on the contact surface of neutral lipids. The free fatty acids released from the TAG contains carboxyl group but is still insoluble in water. Excess amount of free fatty acids causes cytotoxicity (Brookheart et al. 2009), therefore, it should be anchored to coenzyme A or the proteins such as acyl carrier protein and serum albumin. If the organism wants to store much energy in small space (like seed tissue), lipids are more favorable compounds than carbohydrates,

but they have some difficile features as mentioned.

Lipids are highly reduced forms of carbon; this feature confers high calorific value and hydrophobicity at the same time. The hydrophobic lipids especially neutral lipids are necessary to be sheltered from intracellular hydrophilic environment. Generally, the neutral lipids in the cell form globule-like structure called lipid droplet (Murphy and Vance 1999, Murphy 2012). The lipid droplet is thought to be generated from phospholipid bilayer of endoplasmic reticulum (ER) and certain proteins localize at the surface of the lipid droplet (Ohsaki et al. 2014, Pol et al. 2014). The structure of lipid droplet can be reconstituted *in vitro* by simple sonication treatment to mixture of TAG and lecithin, but this artificial lipid droplet is cohesive and unstable (Chen et al. 2004). Addition of recombinant oleosin or caleosin, a well-known lipid droplet protein in plant seed, can improve stability of the artificial lipid droplet (Chen et al. 2004). It is considered that the primary meaning of surface protein of the lipid droplet is to shelter hydrophobic neutral lipids and to maintain the integrity of the particles at the border of hydrophobic and hydrophilic environment. Of course, such scaffold proteins and other diverse proteins on the lipid droplets are possibly related to the metabolic regulation of neutral lipids via lipogenesis and lipolysis, cellular signaling, or membrane trafficking.

The most well studied lipid droplet proteins are perilipin family proteins, identified in mammalian fat tissues, due to its therapeutic importance for obesity and tissue dysfunctions such as hepatic- and myocardial-steatosis (Kimmel et al. 2010). The distribution of the perilipin family proteins on the mammalian lipid droplets differs depending on the tissues. Perilipin1 is dominance in the lipid droplets of adipose tissue, while perilipin2 is secondary abundant in the adipose and the most abundant in cytosolic lipid droplets in liver tissue (Sztalryd and Kimmel 2014). The perilipins can be found especially on the metazoan lipid droplets, but the fungi such as *Saccharomyces*, the other group of opisthokonta, does not utilize the perilipins as the lipid droplet protein (Athenstaedt et al. 1999). Plant, whose linage is far from opisthokonta, has oleosin family protein as the lipid droplet protein, and the amino acid sequence of oleosin does

not have homology to that of perilipin (Chapman et al. 2012). In addition, some novel proteins localized at the lipid droplets are recently demonstrated in other eukaryotic linage (Murphy 2012, Yang et al. 2012). Diversity on the constituent of cytosolic lipid droplets is not high in those organisms; TAG is the main compound. By contrast, diversity on the surface proteins is high. Still, no one can give an exact answer to the questions: why the protein diversity is so high and how the diversity is brought about.

If the ancestral organism obtains the ability to produce TAG and the lipid droplet protein at the initial stage of evolution and if the protein successfully works as regulator of TAG, the protein should be conserved during the evolution, but not in reality. Difference of the surface proteins on the lipid droplets might be responsible for the variety of regulation machinery of storage lipids. For example, adipocytic perilipin1 can interact with at least two lipases through the phosphorylation, but hepatic perilipin2 is not phosphorylated at all (Sztalryd and Kimmel 2014). In multi-cellular organisms, each tissue has their own physiological role as a part of whole body system, so it is not surprising if there are different regulation systems of storage lipids in each tissue. In the case of unicellular organism, the difference of the surface proteins on the lipid droplets may be the result of different strategy on the regulation of storage energy among the species. The number of research on the lipid droplet protein is still not enough for the comparison in whole linage of eukaryote. The further efforts to identify lipid droplet proteins in wide range of species and to characterize its molecular function will give us information about specific strategy on energy storage in different linage.

So far, the evolution of the lipid droplet proteins are discussing in green linage from green algae to land plant rather than metazoan (Liu et al. 2012, Fang et al. 2014, Huang and Huang 2015). While, the functional characterization of the lipid droplet proteins are well progressed in mammalian (Sztalryd and Kimmel 2014). For the fine delineating of strategy on utilization of neutral lipids in various species, both phylogenic analysis and functional characterization of the lipid droplet proteins are required.

Microalgal biomass has attracted great attention as the candidate feedstock for biodiesel (Huang et al. 2010) because of their high biomass productivity per area or per time (Chisti 2007). One of the advantages of microalgae for oil production is that they can accumulate large quantities of neutral lipid (20 – 50% DCW) (Hu et al. 2008) in the lipid droplets (Goold et al. 2015). A marine pennate diatom, *Phaeodactylum tricornutum* is one of the most promising microalgae for biomass production. The biomass of this microalga is expected to be used as feedstock of biodiesel or dietary supplement that contained polyunsaturated fatty acid, eicosapentaenoic acid (EPA) (Fajardo et al. 2007). The *P. tricornutum* also accumulates TAG in the lipid droplets under nitrogen-limited conditions (Guiheneuf et al. 2011, Yang et al. 2013, Abida et al. 2015). In addition, this alga belongs to Stramenopiles in which the lipid droplet proteins were not well studied.

Moellering and Benning (2010) publish the first report about microalgal lipid droplet-localized protein in green alga *Chlamydomonas reinhardtii*. Then, similar proteomic analyses are performed mainly in the green algae (Davidi et al. 2012, Peled et al. 2011, Lin et al. 2012). The homologs of the lipid droplet proteins in microalgae or other organisms are not conserved in the genome of *P. tricornutum*. Therefore, I performed proteomics of the lipid droplets in *P. tricornutum* and tried to characterize the function of the identified protein for the elucidation of the evolution of the lipid droplet-localized protein in Stramenopiles and for the understanding of the strategy on regulation of storage lipid by the lipid droplet proteins.

CHAPTER 1: Identification of a Major Lipid Droplet Protein in a Marine Diatom *Phaeodactylum tricornutum*

1.1. Introduction

Lipid droplets are intracellular compartments that pool lipophilic molecular species. Various kinds of organisms including animals, land plants, yeasts, algae, and bacteria can form lipid droplets in their cells (Murphy and Vance 1999, Murphy 2012). Common features of lipid droplets are as follows: they arise from the endoplasmic reticulum (ER) and are released into the cytosol, they are mainly filled with TAG, and they are surrounded by a phospholipid monolayer derived from the ER membrane and contain specific proteins on their surface (Ohsaki et al. 2014, Pol et al. 2014, illustrated in Figure 1). These proteins play a role as structural proteins to stabilize the lipid droplet, as enzymes for lipid metabolism, and as intracellular membrane trafficking (Murphy and Vance 1999, Martin and Parton 2006, Murphy 2012). Proteomic analyses of the lipid droplets in various organisms have recently been reported (Yang et al. 2012). Although lipid droplets are ubiquitous organelles, their surface proteins are quite diverse; for example, the PAT family proteins on mammalian cytosolic lipid droplets include perilipin, adipophilin, TIP47, S3-12, and OXPAT (Wolins et al. 2006, Brasaemle 2007). In spermatophyta (seed plants), the major proteins on lipid droplets are oleosin family proteins, and they include oleosin, caleosin, and steroleosin (Frandsen et al. 2001, Chapman et al. 2012). Although lipid droplets in mammalian adipocytes and plant seeds have similar roles, the sequences of these two protein families located on the lipid droplet are very low. On the other hand, information about algal lipid droplets and their surface proteins is scarce, and only a few cases have been reported for the model algae. For example, proteins that regulate size of the lipid droplets, i.e., major lipid droplet protein (MLDP), are identified in *Chlamydomonas reinhardtii* (Moellering and Benning 2010, Nguyen et al. 2011) and *Dunaliella salina* (Davidi et al. 2012). Not only cytoplasmic but

also plastidic β-carotene lipid body proteins are analyzed in *Dunaliella bardawil* (Davidi et al. 2014). In an astaxanthin-accumulating alga, *Haematococcus pluvialis*, the surface protein of the lipid droplets termed *Haematococcus* oil globule protein (HOGP) is revealed to be an ortholog of MLDP (Peled et al. 2011). In addition, putative caleosin is discovered to be the main protein in the lipid droplet fraction of *Chlorella* sp. (Lin et al. 2012), as well as caleosin-related *Symbiodinium* lipid droplet protein (SLDP) identified in the endosymbiotic dinoflagellates, *Symbiodinium* (Pasaribu et al. 2014). Moreover, alkenone body-associated proteins are analyzed in the haptophyte alga *Tisochrysis lutea* (Shi et al. 2015).

Lipid droplet proteins in the Stramenopiles have only been analyzed in two species, *Nannochloropsis oceanica* (Vieler et al. 2012) and *Fistulifera* sp. JPCC DA0580, named *F. solaris* (Nojima et al. 2013). Lipid droplet surface protein (LDSP) is identified in *N. oceanica* and is found to have a central hydrophobic domain (Vieler et al. 2012). Nojima et al. (2013) identify five candidates for the lipid droplet proteins in the diatom *F. solaris*.

I focused on the oil-producing diatom *P. tricornutum* and investigated its lipid droplet proteins to understand the mechanism of lipid accumulation. In this study, I firstly isolated the lipid droplets by sucrose gradient centrifugation, and then identified the proteins by performing SDS-PAGE followed by ESI-Q/TOF mass spectrometry of target peptide fragments. Obtained m/z data were processed using the *P. tricornutum* genome-based database search for identification. The sequence of the lipid droplet protein identified was then confirmed by GenBank database search and the presence of similar sequences of lipid droplet-associated proteins in a variety of organisms were suggested through a BLAST search.

1.2. Materials and Methods

1.2.1. Strain and culture condition

Phaeodactylum tricornutum CCAP 1055/6 was used for all experiments. The cells were cultured in a modified Mann and Myers medium (Mann and Myers 1968) as the normal medium. The

composition of the medium is described in Table S1. In the N-deficient culture, I used a N-free medium that did not contain sodium nitrate. The cells were washed with N-free medium three times before inoculation into N-free culture. Cultivation was conducted at 20°C under 200 μmol photons m^{-2} s^{-1} from a continuous white fluorescent lamp. The culture was aerated with filtered air containing 1% (v/v) CO_2. For isolation of the lipid droplets, I used two 1 L Erlenmeyer flasks with 800 mL of medium for cultivation, and 1.6 L of culture medium was used for each experiment. The cells cultured in the standard medium were transferred into the N-free medium and were then cultured for 6 days to induce the formation of lipid droplets.

1.2.2. Lipid droplet isolation

The cells were harvested by centrifugation at 3000 × *g* for 5 min at room temperature and washed using Tris buffer (10 mM Tris-HCl, pH 7.6) with 2% (w/v) NaCl solution. The following procedures were performed on ice. The harvested cells were re-suspended with sucrose buffer (0.25 M sucrose and 1× protease inhibitor cocktail (cOmplete, Roche Diagnostics, Basel, Switzerland) in the Tris buffer), then disrupted using a French press at 1 kpsi (model OS, Constant Systems Ltd., Northants, UK). After the disruption, the unbroken cells and other organelles were removed as a pellet by centrifugation at 50,000 × *g* for 5 min at 4°C. The surface layer of the supernatant containing the lipid droplets was collected into other tubes. Then, 1 mL of 2.5 M sucrose solution was added to 4 mL of the collected supernatant to adjust the sucrose concentration to 0.7 M. I gently poured the Tris buffer on the 0.7 M sucrose solution to make a discontinuous sucrose gradient layer. The tubes were centrifuged again at 50,000 × *g* for 20 min at 4°C. Lipid droplets on the surface of the solution were collected into ten 1.5 mL tubes and then centrifuged at 20,000 × *g* for 10 min at 4°C to remove any remnant buffer at the bottom. The remaining lipid droplets in the ten tubes were gathered into one tube and then re-centrifuged and as much buffer solution was discarded as possible. After the enrichment of lipid droplets, 1

mL of weak detergent buffer (0.2% (v/v) Triton X-100 in the Tris buffer) was added to the tube of lipid droplets and incubated on ice for 10 min to remove the debris. Then, the tube was centrifuged at 20,000 × *g* for 10 min at 4°C and the weak detergent buffer was discarded. After the detergent treatment, the lipid droplets were washed twice with the Tris buffer.

1.2.3. Sample preparation for lipid and protein analysis

Cooled-acetone was added to the lipid droplet fraction and incubated at −20°C overnight. The sample tube was centrifuged at 20,000 × *g* for 10 min at 0°C. The lipid-containing acetone supernatant was collected for UV-visible spectrophotometry and lipid analysis. Furthermore, cooled-ethyl acetate was added to the sample to eliminate any residual oil component from the protein precipitate and incubated at −20 °C for 2 h. The tube was centrifuged and the ethyl acetate supernatant was removed. The precipitated protein fraction was dissolved in 6 μL of lysis buffer (7 M urea, 2 M thiourea, 4% CHAPS, 3% Triton X-100, and 2% SDS). For the protein preparation from the whole cells, lysis buffer was directly added to the harvested cells, incubated on ice for 30 min and centrifuged. The supernatant was used as the protein extract from the whole cells.

1.2.4. UV-visible spectrophotometry and silica-gel thin layer chromatography

The crude lipids from the whole cells were extracted by acetone with sonication. These acetone extracts of the lipid droplets and the whole cells were analyzed using an UV-visible spectrophotometer (UV-1800, Shimadzu, Kyoto, Japan). The absorbance of the 350–750 nm wavelengths was measured to evaluate the extent of contaminations, especially of chlorophylls. After the spectrophotometric analysis, the acetone and ethyl acetate extracts described above were evaporated under a N_2 stream and weighed gravimetrically. The lipid extracts were used for silica-gel thin layer chromatography (TLC).

The lipid extracts were re-dissolved in the measured amounts of solvent to adjust the concentration and following volumes of them were taken to TLC plate with micro syringe. For each lipid extract, 25 μg of crude lipids from the whole cells, 10 μg of the lipid droplet fraction, and 10 μg of TAG standard (triolein) were spotted onto a silica-gel TLC plate (HPTLC Silica gel 60 F_{254}, Merch, Darmstadt, Germany). *n*-Hexane: chloroform 1:1 (v/v) was used as a developing solvent. After development, 20% sulfuric acid was sprayed onto the plate and then the plate was heated to visualize the lipid spots.

1.2.5. SDS-PAGE and Western blotting

A 6-μL aliquot of the protein sample solution from the lipid droplets was mixed with 2 μL of 4× SDS sample buffer (0.25 M Tris-HCl (pH 6.8), 8% SDS, 20% sucrose, and 0.008% bromophenol blue), then 0.8 μL of 500 mM dithiothreitol was added to the mixture and incubated at room temperature for 1 h to denature the proteins. Half of the prepared solution (4.4 μL) was used for proteomic analysis and the other half was used for Western blotting against rabbit antiserum against the large subunit of Rubisco (As-RbcL). A protein sample from the whole cell was also prepared in the same manner.

For the proteomic analysis, protein electrophoresis was performed in Novex 12% Tris-Glycine gel (Thermo Fisher Scientific, Boston, MA, USA). The gel was then fixed with a solution that consisted of 40% MeOH and 10% acetic acid for 15 min and stained using GelCode Blue Stain Reagent (Thermo Fisher Scientific, Boston, MA, USA) for 30 min.

For the Western blotting, protein electrophoresis was performed in c-PAGEL C-12.5L minigel (Atto, Tokyo, Japan) as described previously (Tsuji et al. 2012). Universal rbcL antibody (Agrisera, Vännäs, Sweden) which diluted with blocking buffer at 1:20,000 was used as primary antibody.

1.2.6. Peptide preparation for mass spectrometry

The proteins fractionated by SDS-PAGE were sliced into approximately 1-mm^3 pieces. The gel slices were destained and digested with sequence-grade modified trypsin (Promega, Madison, WI, USA) as described previously (Katayama et al. 2001) with minor modifications. After digestion, the peptides were extracted from the gel pieces with acetonitrile:5 % (v/v) formic acid aqueous solution 1:1 (v/v). The extracted solution was recovered into a vial.

1.2.7. MS analysis and database search

The digested peptides were separated by HPLC with a capillary pump (Agilent 1200 series, Agilent Technologies, Santa Clara, CA, USA) equipped with ZORBAX 300SB-C18 (0.3 mm × 150 mm, Agilent) column. For the elution, mobile phase A consisted of H_2O:acetonitrile 95:5 (v/v) containing 0.1% formic acid, and mobile phase B consisted of H_2O:acetonitrile 10:90 (v/v) containing 0.1 % formic acid. The peptide samples were eluted at 5 μL min^{-1} under the following gradient: ratio of mobile phase B started at 5% and increased to 50% for 60 min, then B ratio elevated quickly to 95% for 1 min and was maintained at 95% for 14 min. The eluted peptides were applied to an electrospray ionization quadrupole time-of-flight (ESI-Q/TOF) system (Agilent 6520 Accurate-Mass QTOF LC/MS). The MS scan range was set to m/z 105–3000 and multi-charged ions (+2, +3, and >+3) were preferentially subjected to MS/MS analysis. The obtained data were exported as Mascot generic files and then each corresponding protein was searched for in the genome database of *P. tricornutum* obtained from JGI (http://genome.jgipsf.org/Phatr2/Phatr2.home.html; *Phaeodactylum tricornutum* v2.0) using Mascot Server (version 2.2.06, Matrix Science, London, UK). A BLASTp search for the identified proteins was performed at NCBI (http://www.ncbi.nlm.nih.gov/) and JGI (http://genome.jgi.doe.g.,ov/) websites. Prediction of the transmembrane helix was performed at TMHMM Server 2.0 (http://www.cbs.dtu.dk/services/TMHMM/, Krogh et al. 2001).

1.2.8. Real-time qRT-PCR

After harvesting the cells, respective samples were immediately frozen with liquid N_2 and kept at −80°C until RNA extraction. A bead beater was used for cell disruption. TRIzol reagent and PureLink RNA Mini Kit (Thermo Fisher Scientific, Boston, MA, USA) were used for the RNA extraction. The qualities of total RNA extracts were checked by MOPS-agarose gel electrophoresis.

I performed qRT-PCR and then conducted the analysis using the comparative C_t method (Livak and Schmittgen 2001). The actin12 gene was used as the housekeeping gene. I used the primer set that was previously designed for actin12 (Siaut et al. 2007). For the detection of mRNA of StLDP, I used the following primers: (F-) 5'-GCCTGGTTTCGTTTCGTTG-3' and (R-) 5'-AAGACGGCGACAATCGGTA-3'. SuperscriptIII Platinum SYBR Green qRT-PCR Kit (Thermo Fisher Scientific, Boston, MA, USA) was used for the preparation of the reaction mixture. StepOnePlus (Applied Biosynthesis, Carlsbad, CA, USA) was used for executing qRT-PCR.

1.3. Results

1.3.1. Isolation of lipid droplets and evaluation of contaminants

The isolated lipid droplet fraction was analyzed by microscopy, spectrophotometry, TLC, and immunological methods (Figure 2). Under the light microscopy, I did not detect any contaminant debris in the isolated lipid droplet fraction (Figure 2A, B). Lipids in the isolated lipid droplet fraction were first extracted with acetone and then with ethyl acetate. Figure 2C shows the UV-visible absorption spectra of acetone extracts from the isolated lipid droplets, chloroplasts, and whole cells. The absorption peaks of the lipid droplet fraction were observed at 448 nm and 474 nm, which correspond to carotenoids. Although an absorption peak corresponding to chlorophyll *a* was observed at 663 nm in the extracts from the chloroplasts and the whole cells,

the peak of A_{663} was well suppressed in the extract from the isolated lipid droplets. These results indicate that chloroplast contamination in the isolated fraction was minimal.

Lipids extracted from the isolated lipid droplets and the whole cells were analyzed by silica-gel TLC (Figure 2D). The TAG spot was observed in extracts from the isolated lipid droplets.

I performed a Western blot analysis using As-RbcL in order to confirm the purity of the lipid droplets (Figure 2E, F). The As-RbcL reacted with the proteins extracted from the whole cells but did not react with the proteins extracted from the isolated lipid droplets (Figure 2E, F).

1.3.2. SDS-PAGE and protein identification

I fractionated the proteins that were extracted from the whole cells and from the isolated lipid droplets with SDS-PAGE (R1–R3) (Figure 3). The molecular mass of the major protein in the lipid droplets of *P. tricornutum* was 49 kDa (gel fraction 4).

Proteins identified in the isolated lipid droplet fraction are shown in Table 1. The protein Phatr48859 was identified in all three replicates in gel fraction 4 and it corresponded with the 49-kDa major band. Thus, Phatr48859 may be one of the abundant proteins on the lipid droplets in *P. tricornutum*. As shown in Supplemental figure S1, the orthologs of Phatr48859 were conserved mainly in Stramenopiles; hence I named this protein "Stramenopile-type lipid droplet protein (StLDP)". The results of BLAST search indicated that StLDP did not share any known functional domain with those registered in the National Center for Biotechnology Information (NCBI) database and did not have sequence homology to any known lipid droplet proteins.

Phatr48778, which includes an acyl-CoA binding site, was identified in all three replicates, suggesting that Phatr48778 plays an important role on the lipid droplets, whereby the acyl-CoA binding site relates to fatty acid metabolism. The other identified proteins, presented in Table 1, may be of minor importance because they were only detected in a single experiment. Phatr54019, which is similar to the heat shock protein 70 (Hsp70), may be a molecular chaperone for proteins

located on the lipid droplets. Phatr45894 and Phatr49981 seemed to undergo redox reactions, but I will not speculate on the substrates of these reactions in this work.

1.3.3. Molecular characteristics of StLDP

Figure 4 shows hydropathy plots of StLDP and representative proteins from lipid droplets; i.e., oleosin of *Arabidopsis thaliana* (Chapman et al. 2012) and LDSP of *Nannochloropsis* sp. (Vieler et al. 2012). Although StLDP and two other comparative proteins were composed of different numbers of amino acids, all these proteins had hydrophobic domains in the central region (222–275 aa of StLDP, 54–128 aa of oleosin, and 72–133 aa of LDSP), despite low similarities in their amino acid sequences.

As a result of a BLAST search on databases in NCBI and the Joint Genome Institute (JGI), I found homologs of StLDP conserved in four diatoms (*Fragilariopsis cylindrus*, *Pseudo-nitzschia multiseries*, *Thalassiosira pseudonana*, *and T. oceanica*) and two other heterokontophytes (a Eustigmatophyte; *Nannochloropsis gaditana*; and a brown alga, *Ectocarpus siliculosus*). Figure 5 shows a multiple alignment of amino acid primary sequences of StLDP and its orthologs. The hydrophobic domains are shown in the red dotted square (222–275 aa in *P. tricornutum* StLDP). This domain consists of 54 amino acid residues, which are mainly hydrophobic, except for proline. Four distinctive proline residues (red arrows) were recognized and I suggest that they make a characteristic motif ($PX_9PX_{10}PX_3P$) in the hydrophobic domain. In addition, there were two conserved domains at the N-terminal and C-terminal regions from the central hydrophobic domains (indicated by black and red two-headed arrows, respectively).

1.3.4. Expression levels of StLDP and sizes of lipid droplets during N-deficient cultivation

To examine whether StLDP expression is induced under N-deficient conditions, I determined the levels of StLDP transcripts by qRT-PCR along with the sizes of lipid droplets (Figure 6). I

speculated that if the StLDP served as a major protein, the lipid droplet surface should be filled with it; therefore, change in the surface area of the lipid droplets should be accompanied with the expression of the StLDP. The StLDP expression levels were upregulated during the N-deficient condition and the extent of its induction ranged from 2.8-folds (1 d after N-deprivation) to 7.1-folds (3 d after N-deprivation) than during N-sufficient conditions. The expression levels reached a peak at 3 d after N-deprivation and then decreased to a steady-state level that was approximately 3- to 4-folds higher than the control. Fluctuations in the expression levels corresponded with the size of the lipid droplets, as I expected. Figure 6 presents the average sizes of the lipid droplets during N-deficiency. The average size of the lipid droplets increased up to 4 d after N-deprivation and reached plateau (Figure 6).

1.4. Discussion

1.4.1. Evaluation of contaminants and lipid contents of the lipid droplet fraction

I disrupted the cells as gently as possible to prevent unnecessary breakage of the lipid droplets and other organelles. If the disruption forces are too intense, the risk of contamination by other organelles increases, particularly because debris and vesicles from various organelles are generated. Moreover, cells of common diatoms possess distinct, hard siliceous frustules; thus, it is difficult to break their cells with mild disruption. In previous studies of the diatom *Fistulifera solaris*., Nojima et al. (2013) adopted bead beating as a disruption method, and they reported that debris of chloroplasts could not be excluded. I disrupted the diatom cells using a French press and then the lipid droplets were isolated using sucrose density gradient centrifugation, based on the method of Ding et al. (2013). Vieler et al. (2012) also used a French press, although at 20 kpsi, to disrupt *Nannochloropsis* cells in order to isolate lipid droplets, whereas I employed 1 kpsi. After fractionation using sucrose density gradient centrifugation, I washed the lipid droplets with a weak detergent to remove small amount of debris and to purify the lipid droplets.

Evaluation of purity is an important step in organelle isolation as it guarantees the quality of the fraction. I performed a Western blot analysis using As-RbcL because it is highly sensitive at detecting the target proteins. Nevertheless, contaminants from organelles other than chloroplast stroma may have been present in the isolated lipid droplet fractions. Better evaluation could be accomplished using antibodies against various other organelle markers. I did not detect any contamination by Rubisco, one of the most abundant proteins in cells.

Acetone extracts of the isolated lipid droplets contained certain carotenoids (Figure 2C). According to previous reports, purified lipid droplets from the other microalgae also contained some carotenoids (Moellering and Benning 2010, Peled et al. 2011, Davidi et al. 2012, Vieler et al. 2012). Whether carotenoids are contaminants or native compounds in isolated lipid droplets has not been concluded. In agreement with previous reports of other microalgal lipid droplets (Moellering and Benning 2010, Davidi et al. 2012, Vieler et al. 2012), the isolated lipid droplets in *P. tricornutum* mainly contained TAG (Figure 2D).

1.4.2. Characterization of the identified lipid droplet proteins

In this study, I identified five proteins from the isolated lipid droplets, and StLDP was the major protein. The orthologs of StLDP were conserved in the four other diatom genomes that have been determined and published: Phatr48778 with an acyl-CoA binding site, and three other proteins Phatr54019, Phatr45894, and Phatr49981. Previously five other proteins were identified as candidates for lipid droplet proteins from the diatom *F. solaris*. (Nojima et al. 2013). More recently, Maeda et al. (2014) identified the protein g4301 (similar to g12504) in *F. solaris* as a diatom-oleosome-associated protein 1 (DOAP1) and they discussed an ER-targeting signal in DOAP1. I searched for orthologous proteins among the proteins encoded by the genome of *P. tricornutum*. Except for protein g6705, orthologs of the other four proteins were also conserved in the genome of *P. tricornutum* (Table 2); however, none of them was found in my isolated lipid droplets.

Shi et al. (2015) noted that they identified coccolith scale associated protein-1 as a result of alkenone body proteomics in *T. lutea* and the homolog of this protein in *P. tricornutum* (Phatr55010, unknown function) was upregulated under nitrogen deprivation in previous transcriptomic analysis (Valenzuela et al. 2012). However, the reported protein, Phatr55010, was not detected in my proteomic analysis.

Chlamydomonas MLDP was more hydrophobic protein than *Arabidopsis* oleosin, mouse perilipin, and ADRP (Moellering and Benning 2010). *Phaeodactylum* StLDP showed higher hydrophobic score on GRAVY index at 0.26 than those of *Chlamydomonas* MLDP at 0.11. Ranking the GRAVY index score on some known lipid droplet proteins is as follows: *Nannochloropsis* LDSP (0.71, AFB75402), *Phaeodactylum* StLDP (0.26, XP_002183367), *Chlamydomonas* MLDP (0.11, XP_001697668), avocado LDAP-1 (-0.10, AGQ04593), *Haematococcus* HOGP (-0.13, ADN95182), *Arabidopsis* oleosin (-0.14, AAA87295), mouse ADRP (-0.28, AEB77763), mouse perilipin (-0.40, NP_783571), and *Auxenochlorella* caleosin (-0.59, AEB77763). Thus, especially the lipid droplet proteins in Stramenopiles, namely LDSP and StLDP seem to have higher hydrophobicity than those of the others.

1.4.3. Hydrophobic region and functional domain of StLDP

StLDP has a hydrophobic domain in the protein central region as well as in oleosin of the plant *A. thaliana* and in LDSP of *Nannochloropsis*. On the other hand, other microalgal lipid droplet proteins, such as MLDP in *Chlamydomonas* and *Dunaliella* and DOAP1 in the *F. solaris*, do not have a hydrophobic domain. In addition, the typical motif ($PX_9PX_{10}PX_3P$), which was conserved among Heterokontophyta, exists in this hydrophobic region (Figure 4). In the hydrophobic domain of oleosin, there is also a conserved proline knot motif (PX_5SPX_3P, where X consists of hydrophobic amino acids) (Tzen et al. 1992). The hydrophobic domain in oleosin makes a hairpin-like loop structure, and the proline knot motif (Abell et al. 2004) is located at the tip of the hairpin loop. The folded-hydrophobic domain can be anchored into the hydrophobic core of

the lipid droplet and this structure enables oleosin to localize on the surface of the lipid droplets. I predicted the presence of a transmembrane region of StLDP using TMHMM Server v. 2.0 (Krogh et al. 2001). There were two predicted transmembrane helices in StLDP of *P. tricornutum*; both were 23 amino acid residues (223–245 aa and 252–274 aa). Both of these predicted helices were located in the central hydrophobic region in StLDP and there is a probability that these two helices make a hairpin structure. However, positions for all of the conservative proline residues did not exist between the helices (i.e., at the tip of the hypothetical hairpin loop), unlike the proline knot in oleosin; therefore, the conservative proline residues may have other roles.

When the gene for the oleosin1 protein was knocked out in *Arabidopsis*, the sizes of the lipid droplets increased, and the efficiency of lipid hydrolysis decreased because of a reduced surface area per volume, and germination was also delayed (Siloto et al. 2006). Furthermore, when LDSP was expressed in the oleosin1 knocked-out mutant, the sizes of the lipid droplets recovered but the TAG degradation rate did not recover completely compared with those in the wild type (Vieler et al. 2012). These results indicate that oleosin not only has a structural function but also plays an important role in lipid metabolism. Concerning the enzymatic activities of oleosin, Parthibane et al. (2012) demonstrated that oleosin3 (OLE3) in peanut has both monoacylglycerol acyltransferase and phospholipase activities. OLE3 has *GXSXG* lipase and HX_4D motifs, and these motifs are important for the enzymatic activities in OLE3. Thus, that oleosin itself is related to the biosynthesis and degradation of plant lipids. In the case of StLDP, *GXSXG* or HX_4D motifs did not exist in the entire amino acid sequence. The N-terminal region from the central hydrophobic domain of StLDP was more variable than the C-terminal region when I compared StLDP orthologs in Heterokontophyta (Figure 5). A short sequence in the N-terminal region, which ranged from 164 to 197 amino acid residues in StLDP of *P. tricornutum*, was conserved among the orthologs (black two-headed arrow). Whilst, approximately the 80 amino acid residues located at the C-terminal region, from the next

hydrophobic domain to amino acid 403 in the StLDP were conserved. Interestingly, I noticed that the sequence from 329 to 402 amino acid residues in the C-terminal region of StLDP (red two-headed arrow) was highly conserved among various microorganisms. The proteins that contained these 73 amino acids as a homologous domain were basically conserved in the Stramenopiles (Heterokonta), and they were also found in the Chlorophyta, *Coccomyxa subellipsoidea* C-169 (NCBI ID, XP_005651106), *Micromonas* sp. RCC-299 (XP_002500436), *Micromonas pusilla* CCMP1545 (XP_003062838), the Rhodophyta, *Chondrus crispus* (XP_005715278), the Cryptophyta, *Guillardia theta* CCMP2712 (XP_005838121), the Haptophyta, *Emiliania huxleyi* (XP_005760304), and in bacterium such as Flavobacterium species. It seems that this domain has some types of function.

1.4.4. Distribution of StLDP and other major lipid droplet proteins in the Stramenopiles

I drew the unrooted tree with the overlapping parts in the orthologs in the Stramenopiles (Figure 7). On this tree, the taxa made the corresponding clades and the orthologs seemed to be kept in this lineage. Thus, I speculated that the ancestral gene of StLDP was obtained at common ancestor of Stramenopiles.

As shown in Figure 5 and Figure S1, the amino acid sequences of three StLDP domains indicated in previous section were well conserved especially in heterokontphyta. Nevertheless, StLDP orthologs were not identified in previous studies of the lipid droplet proteins in *Nannochlotopsis* (Vieler et al. 2012) and *Fistulifera* (Nojima et al. 2013). For example, *Nannochlopsis* has LDSP as the major lipid droplet protein and the orthologs of LDSP were only conserved in the *Nannochloropsis* genus (Vieler et al. 2012). It seemed that *Nannochloropsis* genus independently acquired LDSP gene and utilized it as the major lipid droplet protein.

Even if StLDP orthologs were distributed in the genome of the Stramenopiles, it does not mean that they utilize these orthologs as the major lipid droplet protein. LDSP in the

Nannocchloropsis is a good example. It is therefore possible that other unidentified protein plays a role as a surface protein of the lipid droplet in other taxa than *P. tricornutum*.

1.4.5. Relationship between the expression level of StLDP and the surface area of lipid droplets

The qRT-PCR results indicate that the expression level of StLDP reached a peak at 3 d after N-deprivation, which is very similar to the pattern of growth of the lipid droplets (Figure 6). This was, however, a relatively late response compared with HOGP or MLDP, the green algal lipid droplet proteins. Expression of HOGP reached a maximum level at after 12 h of cultivation in an N-deficient medium (Peled et al. 2011). In the case of *C. reinhardtii*, a maximum expression of MLDP was observed after 24 h of N-deprivation (Moellering and Benning 2010). After 3 d in my experiment, StLDP expression decreased and maintained a steady-state level. Observations with a microscope reveal that the average sizes of the lipid droplets were maximal at 4 d after N-deprivation and maintained thus until 6 d (Figure 6). These results provide indirect evidence that StLDP is a main surface protein on the lipid droplets because the change in expression level corresponded to the change in size of the lipid droplets. A difference in the expression pattern between StLDP and green algal lipid droplet proteins may be driven by a different regulatory mechanism.

1.4.6. Protein transition hypothesis during lipid accumulation

The results presented in Figure 6 indicate that there were at least two stages of formation of the lipid droplets. The first was the early stage, which ranged from inoculation (0 d) to 3 d or 4 d on transcription level or actual lipid droplet growth level, respectively, when the lipid droplets accumulated oils inside. The second was at the late stage after these periods, when the lipid droplets retained their oils. I speculate that the composition or the state of the surface proteins on the lipid droplets changed between these two stages because the proteins that are required for

lipid droplets in each stage were different.

A compositional change in surface proteins of lipid droplets was observed in a study of lipid droplets in mouse adipocytes (Wolins et al. 2003, 2005). According to these reports, TIP47 and S3-12 moved from the cytosol to the surface of nascent lipid droplets during initial fat accumulation. In contrast, perilipin and adipophilin constitutively exist on large or middle-sized lipid droplets and relate to sustaining fat storage and lipolysis.

In this report, I isolated lipid droplets from cells that were cultured for 6 d in N-deficient medium, in other words, I prepared lipid droplet samples at their late stage of formation. Accordingly, I speculate that StLDP has a function for maintenance, distribution, and degradation of the lipids as well as perilipin. In addition, Phatr48778 with an acyl-CoA binding protein, and Phatr54019, which is similar to Hsp70, may play a role to assist the distribution or degradation of TAG in lipid droplets.

CHAPTER 2: Homologous Expression of Lipid Droplet Protein Enhanced Neutral Lipid Accumulation in a Marine Diatom *Phaeodactylum tricornutum*

2.1. Introduction

Proteomic analyses of fractionated lipid droplets have identified the proteins present on these lipid droplets in many organisms (Yang et al. 2012). The perilipin (Plin) and oleosin families of proteins are found as the major proteins on the lipid droplets in mammalian tissues and seed cells of spermatophytes, respectively (Yang et al. 2012). At present, five proteins belong to the Plin protein family (Plin1–5) (Kimmel et al. 2010). Plin1 and Plin4 are mainly distributed in the adipose tissue, Plin2 and Plin3 are ubiquitously expressed in the tissues possessing lipid droplets, and Plin5 is expressed in the oxidative tissues such as heart muscle (Sztalryd and Kimmel 2014). Plin1 and Plin2 are the most abundant proteins of cytosolic lipid droplets in the adipose tissue and the liver, respectively (Sztalryd and Kimmel 2014). The oleosin family comprises three proteins: oleosin, caleosin, and steroleosin (Chapman et al. 2012). Oleosin is a major coat protein on the lipid droplets in seed cells. In the microalgal lipid droplets, homologs of the major lipid droplet protein (MLDP) were found in the green algae *Chlamydomonas reinhardtii* (Moellering and Benning 2010, Nguyen et al. 2011), *Dunaliella salina* (Davidi et al. 2012), and *Lobosphera incisa* (Siegler et al. 2017) through proteomic analysis, and in *Scenedesmus quadricauda* using immunology (Javee et al. 2016). In addition, *Haematococcus* oil globule protein (HOGP), an ortholog of MLDP, was found in the green algae, *Haematococcus pluvialis* (Peled et al. 2011). Moreover, lipid droplet proteomics were conducted in the green algae, *Chlorella* sp. (Lin et al. 2012), endosymbiotic dinoflagellates *Symbiodinium* (Pasaribu et al. 2014), haptophytes *Tisochrysis lutea* (Shi et al. 2015), eustigmatophytes *Nannochloropsis oceanica* (Vieler et al. 2012), and the diatom *Fistulifera* sp. JPCC DA0580 (Nojima et al. 2013). Initially, I performed

proteomic analysis on the lipid droplets isolated from *P. tricornutum* and identified a new lipid droplet protein, namely stramenopile-type lipid droplet protein (StLDP) (Yoneda et al. 2016). Although StLDP was identified as the main protein of the lipid droplets in *P. tricornutum*, its function remains unclear because StLDP does not reveal homology with other known lipid droplet proteins and lacks a predictable catalytic domain.

According to reports on modifying the expression levels of main lipid droplet protein, the upregulation of gene expression led to fat accumulation in certain cases. For example, the adenoviral overexpression of Plin2, a major lipid-droplet-coating protein in liver, caused hepatosteatosis in mice, and the TAG content increased two-fold higher in the liver steatosis tissue when compared with the control (Sun et al. 2012). Increasing TAG amounts and dysfunctional effects were also observed with Plin5 overexpression in the mouse cardiomyocytes (Pollak et al. 2013, Wang et al. 2013). Alternatively, the overexpression of Plin1, a major lipid-droplet-coating protein in the adipose tissue, led to a leaner phenotype and lower adipose depot weight in the transgenic mice when compared with the wild type (WT) mice (Miyoshi et al. 2010).

In a land plant study, Liu et al. (2013) reported that the transgenic rice seeds expressing soybean oleosin exhibited around 1.4-fold higher lipid content than WT; however, the detailed mechanisms facilitating lipid accumulation still remain unclear. Heterologous expression of Plin and oleosin in the yeast, *Saccharomyces cerevisiae*, elevated the neutral lipid levels under radiolabeled palmitic acid feeding conditions (Jacquier et al. 2013). Shemesh et al. (2016) also performed heterologous expression of the green algal HOGP gene in *P. tricornutum* and reported higher total fatty acid content and TAG accumulation. To the best of our knowledge, no reports are available on the homologous expression of the main lipid droplet protein in microalgae.

In this study, I produced *P. tricornutum* mutant that enhanced expression of homologous StLDP gene to determine the function of the lipid droplet protein, and hypothesized that it would facilitate lipid accumulation.

2.2. Materials and Methods

2.2.1. Microalgal strain and culture conditions

Phaeodactylum tricornutum CCAP1052/6 was cultivated at 20 °C with continuous light at 70 µmol photons m^{-2} s^{-1}. Half strength seawater, which prepared using 17 g/L of Coral Pro salt (Red Sea, Eilat, Israel) and enriched with f/2 nutrient (Guillard and Ryther 1962), was used in the strain maintenance and dutring the course of transformation. 4f medium, which contained 8-fold higher nitrate and phosphate concentration than in f/2 was used in main cultivation experiment. I carried out the main cultivation in 200 mL Erlenmeyer flask with 120 mL liquid medium and ambient air was bubbled for agitation.

2.2.2. Construction of plasmids

For the construction of the expression vector of the Stramenopile-type lipid droplet protein (StLDP), first I amplified StLDP gene DNA that fused with histidine (his) -tag and EcoRI /HindIII digestion site by PCR with following primes: (F-) 5'-CGAGAATTCATGCCTTCTTCGAGCAATCC-3' and (R-) 5'-CTGAAGCTTTTAGTGATGGTGGTGATGGTGGCTTGCAGGAACAAGCATGG-3'. In this PCR reaction, the genomic DNA of *P. tricornutum* was used as template. The amplified fragment was digested by corresponding restriction enzymes and ligated into multiple clonig site (MCS) of the plasmid pPha-T1 (Zaslavskaia et al. 2000) with DNA ligation Kit (Takara Bio, Otsu, Japan). The MCS located between fucoxanthin-chlorophyll binding protein (fcp) A promoter and terminator. Thus, the inserted gene in MCS was expressed under the control of fcpA promoter. The expression cassette of *sh ble* gene under the control of fcpB promoter located at the downstream of fcpA/MCS cassette in the pPha-T1. This *sh ble* gene conferred zeosin resistance to the diatom cell. Professor Peter Kroth, Universität Konstanz, kindly gave the pPha-T1 plasmid for me. Finally, I confirmed the DNA sequence of inserted gene by DNA

sequencing using BigDye Cycle Sequencing Kit (Thermo Fisher Scientific, Boston, MA, USA) and 3130 Genetic Analyzer (Applied Biosystems, Carlsbad, CA, USA).

2.2.3. Transformation of diatom

The diatom cells were transformed by the protocol described in Zaslavskaia et al. (2000) with minor modification. Approximately 7×10^7 cells were spread on an agar plate and bombarded using a BioRad Biolistic PDS-1000/He Particle Delivery System (BioRad, Hercules, CA, USA) with 1350 psi rupture disc. Gold particles (1.0 μm diameter) that coated with 3 μg of circular plasmid DNA, 0.1M spermidine, and 2.5M $CaCl_2$ were bombarded twice per plate. After an overnight recovery culture, the bombarded diatom cells were then cultivated on a selection plate that contained 50 μg/mL zeocin.

Integration of his-tagged StLDP into the genomic DNA was confirmed by PCR with following His-tagged StLDP specific primers: (F-) 5'-CGAGAATTCATGCCTTCTTCGAGCAATCC-3' and (R-) 5'-TTAGTGATGGTGGTGATGGTG-3'. In addition, the gene expression of his–tagged StLDP was confirmed by RT–PCR with same primer set.

2.2.4. Cultivation experiment in nitrogen deficient medium

Wild type (WT) and his-tagged StLDP expressing strain (His1-22-8; H8) were pre-cultured in 4f medium for 1 week and inoculated in fresh 4f medium. The initial cell concentrations were adjusted to 0.15 at an optical density of 750 nm. The strains were cultivated in nitrogen-sufficient medium for 4 days, and were then transferred into nitrogen-deficient 4f medium that laced a nitrogen source. Before the transfer, I washed the cells twice with nitrogen-deficient medium. The cultivation under nitrogen-deficient condition was carried out for 6 days.

2.2.5. Dry cell weight measurement and lipid analysis

For DCW measurements, cells in 10 mL culture broth were harvested on the preweighted GF/C glass filter, and were dried at 55 °C in an oven. The dried biomass residues on the filter were then gravimetrically measured.

I extracted the crude lipid using Folch method (Folch et al. 1957). The wet biomass pellet obtained by centrifugation of 50 mL of culture broth was used directly for chloroform/methanol extraction. The amount of the crude lipid extracts was measured gravimetrically after the extraction. The composition of neutral and polar lipids was determined using silica gel column chromatography with Silica Gel 60 (Merck, Darmstadt, Germany) as a support. The crude lipids were eluted first using chloroform (four times the volume of the column bed), followed by the same volume of methanol. The chloroform fraction contained neutral lipids, mainly TAG, whereas the methanol fraction contained polar lipids such as phospholipids and glycolipids.

2.2.6. RNA extraction and qRT–PCR

The RNA extraction procedure and qRT–PCR for the quantification of StLDP expression were performed as per our previous report (Yoneda et al. 2016). In this study, we used TRIzol reagent (Thermo Fisher Scientific, Boston, MA, USA) and RNeasy Mini Kit (Qiagen, Hilden, Germany) for total RNA extraction. A PrimeScript RT Reagent Kit with gDNA Eraser (Takara Bio, Shiga, Japan) was used to eliminate residual genomic DNA and cDNA synthesis, and SYBR Premix ExTaq II (Tli RNaseH Plus) (Takara Bio, Shiga, Japan) was used for the two-step real-time qRT–PCR.

2.2.7. Quantification of lipid droplet size and number

Microscopic image was captured with Olympus BX53 microscopy system (Olympus, Center

Valley, PA, USA). The lipid droplet was stained with Nile red (Wako, Osaka, Japan) and observed under fluorescent microscopy equipped with BNA fluorescent mirror (green filter, excitation: 475–495 nm, absorption: 510–550). The captured images were analyzed with ImageJ (Abramoff et al. 2004). The green fluorescent dots derived from Nile red-stained lipid droplets were numbered and the size of each fluorescent area was measured by the ImageJ. The diameters of lipid droplet were calculated from the area and the number of lipid droplet per cell was manually counted from the processed image.

2.3. Results

2.3.1. Growth curve, DCW, lipid content, and expression level of StLDP in wild type and mutant

To determine the function of StLDP, Wild type (WT) and his-tagged StLDP expressing strain (H8) were cultivated in nitrogen-sufficient medium for 4 days and in nitrogen-deficient medium for 6 days. Figure 8A presents the growth curve of these strains and Figure 8B reveals the DCW and lipid amounts at the end of cultivation. No significant differences were seen in the growth, DCW, and crude lipid amount between the strains. Figure 8C represents the expression level of StLDP at Days 0, 3, and 6 in nitrogen-deficient cultivation. The expression of StLDP in H8 was 57-fold higher than that in WT at Day 0; however the enhanced of StLDP expression in H8 decreased at Day 3 to a slight level that was 1.2-fold higher than the wild type, and finally reached to the same level as the WT at Day 6. Gene expression of the introduced his-tagged StLDP under the control of fcpA promoter was attenuated after the prolonged cultivation period under nitrogen starvation.

2.3.2. Lipid composition in wild type and mutant

Figure 9 indicates the proportion of neutral and polar lipid in WT and H8 mutant at Days 0 and 6 in nitrogen-deficient condition. The composition of neutral lipids was similar in both strains at

Day 0 (33.2±1.3% and 33.4±1.4% in WT and H8, respectively; Figure 9A). A significant increase on neutral lipid content was observed at Day 6 (45.3 ± 2.8% and 53.5 ± 2.3% in WT and H8, respectively; Figure 9B; P = 0.009, Student's t-test, n = 3). On the contrarily the composition of polar lipids significantly decreased in the H8 mutant when compared with WT (Figure 9B; P = 0.035, Student's t-test, n = 3). This suggested that the homologous expression of StLDP promoted the accumulation of neutral lipids.

2.3.3. Microscopic observation during the cultivation in nitrogen deficient medium

Figure 10 presents the microscopic images of WT and H8 mutant at Days 0, 2, and 6 in the nitrogen-deficient condition. At Day 0, just before the inoculation into the nitrogen-deficient medium, none of strains form lipid droplets in the cells (Figure 10A). This observation revealed that the overexpression of StLDP per se did not trigger for the formation of lipid droplets. Even at Day 1, scanty lipid droplets were seen; however, after Day 2, the lipid droplets were observed in WT and H8 mutant (Figure 10B), revealing that the timing of induction of lipid droplet formation was same in both strains. At the end of cultivation (Day 6), I could observe large lipid droplets (Figure 10C), suggesting that lipid droplet fused with each other as the result of attenuation of StLDP expression in the H8 strain under prolonged cultivation period under nitrogen starvation.

2.3.4. The lipid droplet diameter and the number of lipid droplet per cell

As shown in Figure 9B, the neutral lipid composition increased in the H8 mutant at the final day. The expression level of StLDP was strongly enhanced in the H8 at Day 0, before the cultivation in nitrogen-deficient medium (Figure 8C); however, the neutral lipid accumulation and lipid droplet formation was not observed at the Day 0 (Figure 9A and 10A). Thus, the major effect of the StLDP expression occurred after the re-inoculation into the nitrogen-deficient medium. I

speculated that the major effect was occurred at the initial stage of nitrogen deprivation because the expression of introduced his-tagged StLDP decreased to the same level as the WT at later stage (Day 6, Figure 8C). Herein, I focused on the size and number of lipid droplets, especially at Day 2, the initial stage of lipid droplet formation.

Figure 4A and B presents the distribution of the diameter of each lipid droplets at Days 2 and 6. At Day 2, the distribution of lipid droplet diameter was similar in WT and H8 mutant (Figure 11A), and the average of the diameter was not different in both strains (1.26 ± 0.47 μm and 1.36 ± 0.52 μm in WT and H8, respectively). Alternatively, the proportion of larger lipid droplet increased in H8 mutant at Day 6 (Figure 11B) and reflected higher neutral lipid content in H8 mutant at Day 6 (Figure 9B). Figure 4C reveals the number of lipid droplet per cell at Day 2. In WT, almost all single cells (97.0%) formed one or two lipid droplet(s), whereas in the H8 strain, the proportion decreased to 78.8% and the proportion of the cells that formed three or four lipid droplets increased (15.1% and 6.0%, respectively). In particular, on the size distribution, the lipid droplet was similar; however, the number of lipid droplets per cell changed between the strains at Day 2. These observations suggested that the enhanced StLDP expression increased the number of lipid droplet per cell at initial nitrogen-deficient period, and led to promote the neutral lipid accumulation.

2.4. Discussion

2.4.1. Growth and expression level of StLDP in mutant

As shown in Figure 1A, the expression of his-tagged StLDP in the H8 mutant did not lead to growth inhibition; however, overexpression of StLDP in the H8 mutant was restricted to at Day 0 (Figure 8C). This was explained by the attenuation of expression by the fcpA promoter under nitrogen deficiency. A transcriptomic study of *P. tricornutum* demonstrated that LHCF1 gene (also known as fcpA) and several genes related to the photosynthesis and pigment biosynthesis were repressed during nitrogen deprivation (Alipanah et al. 2015). To improve the expression

level under nitrogen deprivation, Shemesh et al. (2016) developed a new promoter of diacylglycerol acyltransferase 1 (DGAT1) gene from *P. tricornutum*; however, they reported that although pDGAT1 promoted gene expression under nitrogen deprivation, the expression levels were still lower than that the other strong promoters (e.g., fcpA). Utilization of pDGAT1 or other promoters under nitrogen deprivation require for further investigation.

2.4.2. Accumulation of neutral lipid in nitrogen deficient condition and function of StLDP

Despite the restriction of overexpression by fcpA promoter, the significant differences were observed in lipid composition (Figure 9). In this study, the percentage of neutral lipid content was increased by 18% in the H8 mutant when compared with WT (Figure 9B). Elevation of neutral lipid due to the expression of lipid droplet protein has often been reported in the previous studies (Sun et al. 2012, Pollak et al. 2013, Wang et al. 2013). The lipid droplet-coating proteins likely function to protect storage lipid (i.e., TAG) from the cytosolic lipases. Thus, one of the reasons for the oil accumulation induced by StLDP overexpression could be due to the enhanced protection ability and the interruption of hydrolyzes by the lipases (Miyoshi et al. 2010, Pollak et al. 2013).

In transgenic mice, the overexpression of Plin1 led to a leaner phenotype and lower fat accumulation in the adipocytes. This was explained by the differentiation of white adipose tissue to a more energy-consuming brown adipose-like tissue that led to higher energy expenditure, upregulation of mitochondrial fatty acid β-oxidation, and downregulation of lipogenic genes (Sawada et al. 2010, Miyoshi et al. 2010). Alternatively, the overexpression of Plin5 in mouse heart tissue slightly downregulated the mitochondrial medium chain acyl-CoA dehydrogenase that is related to fatty acid β-oxidation (Wang et al. 2013).

According to Jacquier et al. (2013), heterologous expression of Plin family proteins and oleosin in the yeast, *S. cerevisiae*, led to increased TAG levels. Deletion mutants of

phosphatidate phosphatase, PAH1, which catalyzes the dephosphorylation of phosphatidate during the glycerolipid biosynthesis, could not form lipid droplets in the cell, and TAG and sterol ester (STE) existed at the bilayer of the ER membrane in the *pah1Δ* yeast mutant (Jacquier et al. 2013). Irregular accumulation of neutral lipids on the ER membrane is not compatible with lipogenic enzymes as they change the physical properties of the ER membrane and the products remain at the reaction site. The expression of Plins and oleosin in the *pah1Δ* mutant led to the relocation of these neutral lipids into the lipid droplet and enhanced the TAG and STE biosynthesis (Jacquier et al. 2013). The authors concluded that the accumulated neutral lipids on the ER membrane were released by the expression of Plin and oleosin that facilitated the sequestration of synthesized neutral lipid product (i.e., TAG and STE) from the ER to the lipid droplet.

Previous reports have revealed that changes in the neutral lipid content induced by altered expression of lipid droplet proteins are necessary for three essential functions: (1) to form a physical barrier on the lipid droplet surface in order to prevent the degradation of neutral lipid from lipases; (2) to modulate the enzymatic activity related to lipogenesis and lipolysis; and (3) to facilitate the sequestration of neutral lipid products into lipid droplets.

The expression of StLDP in H8 mutant was 57-fold higher than that in WT in nitrogen-sufficient condition (Figure 8C); however, the H8 mutant did not form lipid droplet under nitrogen sufficient condition (Figure 10A), and the lipid composition did not differ from WT (Figure 9A). From these results, at least under nitrogen-sufficient condition, StLDP itself should not trigger either lipogenesis or lipolysis. After cultivation in nitrogen-deficient medium, the percentage composition of neutral lipids was increased in H8 mutant (Figure 9B), and the proportion of the cells that had more than three lipid droplets in a single cell at Day 2 was significantly increased in the H8 mutant (Figure 11C). Thus, I hypothesized that StLDP facilitated sequestration of TAG at the initial stage of lipid droplet formation and led to an increase of the number of lipid droplets in the H8 mutant. At the end of the cultivation (Day 6),

the proportion of large lipid droplets increased in the H8 mutant (Figure 11B). I speculated that tiny lipid droplets generated at Day 2 fused each other due to a decrease of coating protein caused by the attenuation of StLDP expression during nitrogen deficiency (Figure 8C), producing large lipid droplets observed at Day6 in the H8 mutant. Prolonged upregulation of StLDP gene in nitrogen-deficient culture may enhance further lipid accumulation through the physical barrier effects of lipid-droplet-coating proteins. Further studies are necessary to determine whether StLDP is involved in the regulation of lipogenic or lipolytic enzymes in the nitrogen-deficient conditions.

General Discussion

The major importance of this study consists of the finding of novel abundant lipid droplet protein present in marine diatom *P. tricornutum* and the first demonstration of homologous expression of lipid droplet protein in phycology. From the result in homologous expression, it was suggested that StLDP facilitated sequestration of TAG at the initial stage of lipid droplet formation. However, the detail machinery of StLDP for oil metabolism in lipid droplet is still unclear.

In the latest study by Huang and Huang in 2015, a thousand genes of oleosins that conserved in green algae to seed plant are classified into five lineages: P (primitive), U (universal), SL (seed specific, low molecular weight), SH (seed specific, high molecular weight), T (tapetum specific). Among them, SL-, SH-, and T-oleosins work as the major protein in the lipid droplets. All vascular plants possess U-oleosins, which derived from P-oleosin; nevertheless, the expressions of the U-oleosins are very low in various tissues in the land plant and they do not serve as primary surface proteins of the lipid droplets. In addition, U-oleosins have highly conserved C-terminal region. The authors mention that the U-oleosins may have indispensable function for the life in their C-terminal region, because their genes are preserved in all land plant for 200 million years in their evolution. In the case of StLDP, the orthologs were distributed among the genomes of Stramenopiles and C-terminal flanking region of the central hydrophobic domain was conserved as well. It was considered that the lipid droplet-localized proteins in some cases evolved as the results of gene fusion between the functional gene and the amino acid motif required for localization to the lipid droplet.

I could observe the neutral lipid accumulation by the homologous expression of StLDP. It was suggested that at least StLDP had the ability as the barrier from cytosolic lipases. However, the regulation machinery of neutral lipids by StLDP is still unknown and nobody knows the advantage of possessing StLDP. Perhaps, the initial reaction of lipolysis that catalyzed by lipases or the final reaction to produce glycerolipids should be regulated the accumulation of storage

lipids through the StLDP. Otherwise, other dynamic pathway such as membrane transport might relate on the regulation of storage lipids. The interaction between StLDP and other functional proteins might be regulated through the phosphorylation and protein interaction as well in perilipin1. Conversely, StLDP might work only as physical barrier to the lipases. In this case, proteasome system might regulate StLDP degradation through the ubiquitination.

Stramenopiles is diverse taxonomical group that contains oleaginous organisms such as diatom, *Nannochloropsis*, and Thraustochytrids; thus, the surface proteins in the lipid droplets should be analyzed for better understanding on the regulation of neutral lipids. The extensive research on the lipid droplet proteins are only performed in green linage and Opistokonta so far. I expect that Stramenopile lineage will also be focused as the research target on the lipid droplet proteins. To figure out the diversity of the lipid droplet proteins and the strategy on the regulation of storage energy among the species, further analyses on the identification of the lipid droplet proteins in wide range of species, the phylogenic analysis, and the characterization of regulatory machinery are necessary in the future.

ACKNOWLEDGEMENTS

Firstly, I would like to express my sincere gratitude to my supervisors Professor Makoto M. Watanabe and Professor Iwane Suzuki for their continuous encouragement and appropriate guidance in my study life in University of Tsukuba. Their diverse and deep knowledge and perspective raise me up all the time. It all started when I took the class of Prof. Watanabe at my bachelor degree. I greatly appreciate him because his lecture opened the door for me to enter this scientific field. I am also deeply indebted to Prof. Suzuki for accepting me as a doctoral student of Laboratory of Plant Physiology and Metabolism after the retirement of Prof. Watanabe. His comprehensive and kind supports enable me to undertake my research.

Next, I would also like to express my special appreciation to Assistant Professor Masaki Yoshida for his direct technical guidance, academic advices, and various supports in the research works. Thanks to his accurate designations and warm-hearted nature, I could spend all my graduate school life without worries.

I also appreciate Doctors Yoshinori Tsuji, Hiroya Araie, and Masato Baba for their experimental support and helpful suggestions, and colleagues and staffs in the Laboratory of Plant Physiology and Metabolism, M. M. Watanabe Laboratory, Plant Diversity and Evolutionary Cell Biology Laboratory in the University of Tsukuba for a lot of active discussions and supports.

I also grateful to Professor Tsuneyoshi Kuroiwa and research fellows in the Laboratory of Cell Biology in Rikkyo University for giving me permission to use the MALDI-TOF mass spectrometer for preliminary experiments on lipid droplet proteomics.

Finally, I would like to express my profound thanks to my parents for providing never-failing support and encouragement throughout all my study life in the University of Tsukuba.

KOHEI YONEDA

REFERENCES

Abell, B. M., Hahn, M., Holbrook, L. A. and Moloney, M. M. (2004) Membrane topology and sequence requirements for oil body targeting of oleosin. Plant J. 37: 461-470.

Abida, H., Dolch, L. J., Mei, C., Villanova, V., Conte, M., Block, M. A., et al. (2015) Membrane glycerolipid remodeling triggered by nitrogen and phosphorus starvation in *Phaeodactylum tricornutum*. Plant Physiol. 167: 118-136.

Abramoff, M. D., Magalhaes, P. J. and Ram, S.J. (2004) Image processing with ImageJ. Biophotonical International 11: 36-42.

Alipanah, L., Rohloff, J., Winge, P., Bones, A. M. and Brembu, T. (2015) Whole-cell response to nitrogen deprivation in the diatom *Phaeodactylum tricornutum*. J. Exp. Bot. 66: 6281-6296.

Athenstaedt, K., Zweytick, D., Jandrositz, A., Kohlwein, S. D. and Daum, G. (1999) Identification and characterization of major lipid particle proteins of the yeast *Saccharomyces cerevisiae*. J. Bacteriol. 181: 6441-6448.

Brasaemle D. L. (2007) The perilipin family of structural lipid droplet proteins: stabilization of lipid droplets and control of lipolysis. J. Lipid. Res. 48: 2547-2559.

Brookheart, R. T., Michel, C. I. and Schaffer, J. E. (2009) As a matter of fat. Cell Metab. 10: 9-12.

Chapman, K. D., Dyer, J. M. and Mullen, R. T. (2012) Biogenesis and functions of lipid droplets in plants. J. Lipid. Res. 53: 215-216.

Chen, M. C. M., Chyan, C., Lee, T. T., Huang, S-H. and Tzen, J. T. C. (2004) Constitution of stable artificial oil bodies with triacylglycerol, phospholipid, and caleosin. J. Agric. Food Chem. 52: 3982-3987.

Chisti Y. (2007) Biodiesel from microalgae. Biotechnol. Adv. 25: 294-306.

Davidi, L., Katz, A. and Pick, U. (2012) Characterization of major lipid droplet proteins from *Dunaliella*. Planta 236:19-33.

Davidi, L., Levin, Y., Ben-Dor, S. and Pick, U. (2015) Proteomic analysis of cytoplasmatic and plastidic

β-carotene lipid droplets in Dunaliella bardawil. Plant Physiol. 167: 60-79.

Ding, Y., Zhang, S., Yang, Li., Na H., Zhang, P., Zhang, H. and Wang, Y. et al. (2013) Isolating lipid droplets from multiple species. Nat. Protoc. 8: 43-51.

Fahy, E., Subramaniam, S., Murphy, R. C., Nishijima, M., Raetz, C. R. H., Shimizu, T. et al. (2009) Update of the LIPID MAPS comprehensive classification system for lipids. J. Lipid Res. S9-S14.

Fajardo, A. R., Cerdan, L. E., Medina, A. R., Fermamdez, F. G. A., Moreno, P. A. G. and Grima, E. M. (2007) Lipid extraction from the microalga *Phaeodactylum tricornutum*. Eur. J. Lipid Sci. Technol. 109: 120-126.

Fang, Y., Zhu, R-L. and Mishler, B. D. (2014) Evolution of oleosin in land plants. PLoS ONE 9: e103806.

Folch, J., Lee, M. and Stanley, G. H. S. (1957) A simple method for the isolation and purification of total lipids from animal tissues. J. Biol. Chem. 226: 497-509.

Frandsen, G. I., Mundy, J. and Tzen, J. T. C. (2001) Oil bodies and their associated proteins, oleosin and caleosin. Physiol.Plantarum 112: 301-307.

Goold, H., Beisson, F., Peltier, G. and Li-Beisson, Y. (2015) Microalgal lipid droplets: composition, diversity, biogenesis and functions. Plant Cell Rep. 34: 545-555.

Guiheneuf, F., Leu, S., Zarka, A., Khozin-Goldberg, I., Khalilov, I., and Boussiba, S. (2011) Cloning and molecular characterization of a novel acyl-CoA: diacylglycerol acyltransferase 1-like gene (PtDGAT1) from the diatom *Phaeodactylum tricornutum*. FEBS J. 278: 3651-3666.

Guillard, R. R. L. and Ryther, J. H. (1962) Studies of marine planktonic diatoms. I. *Cyclotella nana* Hustedt and *Detonula confervaceae* (Cleve) Gran. Can. J. Microbiol. 8: 229-239

Hu, Q., Sommerfeld, M., Jarvis, E., Ghirardi, M., Posewitz, M., Seibert, M. et al. (2008) Microalgal triacylglycerols as feedstocks for biofuel production : perspectives and advances. Plant J. 54: 621-639.

Huang, G., Chen, F., Wei, D., Zhang, X., and Chen, G. (2010) Biodiesel production by microalgal biotechnology. Appl. Energ. 87: 38-46.

Huang, M-D. and Huang, A. H. C. (2015) Bioinformatics reveal five lineages of oleosins and the mechanism of lineage evolution related to structure/function from green algae to seed plants. Plant Physiol. 169: 453-470.

Jacquier, N., Mishra, S., Choudhary, V. and Schneiter, R. (2013) Expression of oleosin and perilipins in yeast promotes formation of lipid droplets from the endoplasmic reticulum. J. Cell Sci. 126: 5198-5209.

Javee, A., Sulochana, S. B., Pallissery S. J. and Arumugam, M. (2016) Major lipid body protein: A conserved structural component of lipid body accumulated during abiotic stress in *S. quadricauda* CASA-CC302. Front. Energ. Res. 4: 37.

Katayama, H., Nagasu, T. and Oda, Y. (2001) Improvement of in-gel digestion protocol for peptide mass fingerprinting by matrix-assisted laser desorption/ionization time-of-flight mass spectrometry. Rapid Commun.Mass Spectrom. 15:1416-1421.

Kimmel, A. R., Brasaemle, D. L., McAndrews-Hill, M., Sztalryd, C. and Londos, C. (2009) Adoption of PERILIPIN as a unifying nomenclature for the mammalian PAT-family of intracellular lipid storage droplet proteins. J. Lipid Res. 51: 468-471.

Krogh, A., Larsson, B., Heijne, G. V. and Sonnhammer, E. L. L. (2001) Predicting transmembrane protein topology with a Hidden Markov Model: Application to complete genomes. J. Mol. Biol. 305: 567-580.

Lin, I., Jiang, P., Chen, C. and Tzen, J. T. C. (2012) A unique caleosin serving as the major integral protein in oil bodies isolated from *Chlorella* sp. cells cultured with limited nitrogen. Plant Physiol.Biochem. 61:80-87

Liu, W. X., Liu, H. L. and Qu, L. Q. (2013) Embryo-specific expression of soybean oleosin altered oil body morphogenesis and increased lipid content in transgenic rice seeds. Theor. Appl. Genet. 126: 2289-2297.

Liu, Q., Sun, Y., Su, W., Yang, J., Liu, X., Wang, Y. et al. (2012) Species-specific size expansion and molecular evolution of the oleosins in angiosperms. Gene 509: 247-257.

Livak, K. J. and Schmittgen, T. D. (2001) Analysis of relative gene expression data using real-time quantitative PCR and the 2(-CΔΔ(T)). Methods 25: 402-408.

Maeda, Y., Sunaga, Y., Yoshino, T. and Tanaka, T. (2014) Oleosome-associated protein of the oleaginous diatom *Fistulifera solaris* contains an endoplasmic reticulum-targeting signal sequence. Mar. Drugs 12: 3892-3903.

Mann, J. E. and Myers, J. (1968) On pigments, growth, and photosynthesis of *Phaeodactylum tricornutum*. J. Phycol. 4: 349-355.

Martin, S. and Parton, R. G. (2006) Lipid droplets: a unified view of a dynamic organelle. Nat.Rev. Mol. Cell.Bio. 7: 373-378.

Miyoshi, H., Souza, S. C., Endo, M., Sawada, T., Perfield II, J. W., Shimizu, C., et al. (2010) Perilipin overexpression in mice protects against diet-induced obesity. J. Lipid Res. 51: 975-982.

Moellering, E. R. and Benning, C. (2010) RNA interference silencing of a major lipid droplet protein affects lipid droplet size in *Chlamydomonas reinhardtii*. Eukaryot. Cell 9: 97-106.

Murphy, D. J. and Vance, J. (1999) Mechanisms of lipid-body formation. Trends. Biochem. Sci. 24: 109-115.

Murphy, D. J. (2012) The dynamic roles of intracellular lipid droplets: from archaea to mammals. Protoplasma 249: 541-585.

Nguyen, H. M., Baudet, M., Cuine, S., Adriano, J. M., Barthe, D., Billon, E. et al. (2011) Proteomic profiling of oil bodies isolated from the unicellular green microalga *Chlamydomonas reinhardtii*: With focus on proteins involved in lipid metabolism. Proteomics 11:4266-4273.

Nojima, D., Yoshino, T., Maeda, Y., Tanaka, M., Nemoto, M. and Tanaka, T. (2013) Proteomics analysis of oil body associated proteins in the oleaginous diatom. J. Proteome res.12: 5293-5301.

Ohsaki, Y., Suzuki, M. and Fujimoto, T. (2014) Open questions in lipid droplet biology. Chem. Biol. 21: 86-96.

Parthibane, V., Rajakumari, S., Venkateshwari, V., Iyappan, R. and Rajasekharan, R. (2012) Oleosin is

bifunctional enzyme that has both monoacyltransferase and phospholipase activities. J. Biol.Chem. 287: 1946-1954.

Pasaribu, B., Lin, I. P., Tzen, J. T. C., Jauh, G. Y., Fan, T. Y., Ju, Y. M., et al. (2014) SLDP: a novel protein related to caleosin is associated with the endosymbiotic *Symbiodinium* lipid droplets from *Euphyllia glabrescens*. Mar. Biotechnol. 16: 560-571.

Peled, E., Leu, S., Zarka, A., Weiss, M., Pick, U., Khozin-Goldberg, I., et al. (2011) Isolation of a novel oil globule protein from the green alga *Haematococcus pluvialis* (Chlorophyceae). Lipids 46: 851-861.

Pol, A., Gross, S. P., and Parton, R. G. (2014) Biogenesis of the multifunctional lipid droplet: Lipids, proteins, and sites. J. Cell Biol. 204: 635-646.

Pollak, N. M., Schweiger, M., Jaeger, D., Kolb, D., Kumari, M., Schreiber, R., et al. (2013) Cardiac-specific overexpression of perilipin 5 provokes severe cardiac steatosis via the formation of a lipolytic barrier. J. Lipid Res. 54: 1092-1102.

Sawada, T., Miyoshi, H., Shimada, K., Suzuki, A., Okamatsu-Ogura, Y., Perfield II, J. W. et al. (2010) Perilipin overexpression in white adipose tissue induces a brown fat-like phenotype. PLoS ONE 5: e14006.

Shemesh, Z., Leu, S., Khozin-Goldberg, I., Didi-Cohen, S., Zarka, A. and Boussiba, S. (2016) Inducible expression of Haematococcus oil globule protein in the diatom Phaeodactylum tricornutum: Association with lipid droplets and enhancement of TAG accumulation under nitrogen starvation. Algal Res. 18: 321-331.

Shi, Q., Araie, H., Bakku, R. K., Fukao, Y., Rakwal, R., Suzuki, I., and Shiraiwa, Y. (2015) Proteomic analysis of lipid body from the alkenone-producing marine haptophyte alga *Tisochrysis lutea*. Proteomics. *in press*.

Siaut, M., Heijde, M., Mangogna, M., Montsant, A., Coesel, S., Allen, A. et al. (2007) Molecular toolbox for studying diatom biology in *Phaeodactylum tricornutum*. Gene 406: 23-35.

Siloto, R. M., Findlay, K., Lopez-Villalobos, A., Yeung, E. C., NykiforukC, L. and Moloney, M. M. (2006) The accumulation of oleosins determines the size of seed oilbodies in *Arabidopsis*. Plant Cell 18: 1961-1974

Sun, Z., Miller, R. A., Patel, R. T., Chen, J., Dhir, R., Wang, H., et al. (2012) Hepatic Hdac3 promotes gluconeogenesis by repressing lipid synthesis and sequestration. Nat. Med. 18: 934-942.

Sztalryd, C., and Kimmel, A. R. (2014) Perilipins: Lipid droplet coat proteins adapted for tissue-specific energy storage and utilization, and lipid cytoprotection. Biochimie 96: 96-101.

Tsuji, Y., Suzuki, I., and Shiraiwa, Y. (2012) Enzymological evidence for the function of plastid-located pyruvate carboxylase in the haptophyte alga *Emiliania huxleyi*: a novel pathway for the production of C_4 compounds. Plant Cell Physiol. 53: 1043-1052.

Tzen, J. T. H., Lie, G. C., and Huang, A. H. C. (1992) Characterization of the charged components and their topology on the surface of plant seed oil bodies. J Biol. Chem. 267: 15626-15634.

Valenzuela, J., Mazurie, A., Carlson, R. P., Gerlach, R., Cooksey, K. E., Peyton, B. M., et al. (2012) Potential role of multiple carbon fixation pathway during lipid accumulation in *Phaeodactylum tricornutum*. Biotechnol. Biofuels 5: 40.

Vieler, A., Brubaker, S. B., Vick, B. and Benning, C. (2012) A Lipid droplet protein on *Nannochloropsis* with functions partially analogous to plant oleosins. Plant Physiol. 158: 1562-1569.

Wang, H., Sreenivasan, U., Gong, D., O'Connell, K. A., Dabkowski, E. R., Hecker, P. A., et al. (2013) Cardiomyocyte-specific perilipin 5 overexpression leads to myocardial steatosis and modest cardiac dysfunction. J. Lipid Res. 54: 953-965.

Wolins, N. E., Skinner, J. R., Schoenfish, M. J., Tzekov, A., Bensch, K. G. and Bickel, P. E. (2003) Adipocyte protein S3-12 coats nascent lipid droplets. J. Biol. Chem. 278: 37713-37721.

Wolins, N. E., Quaynor, B. K., Skinner, J. R., Schoenfish, M. J., Tzekov, A. and Bickel, P. E. (2005) S3-12, Adipophilin, and TIP47 package lipid in Adipocytes. J. Biol. Chem. 280: 19146-19155.

Wolins, N. E., Brasaemle, D. L. and Bickel, P. E. (2006) A proposed model of fat packaging by

exchangeable lipid droplet proteins. FEBS Lett. 580: 5484-5491

Yang, L., Ding, Y., Chen, Y., Zhang, S., Huo, C., Wang, Y., et al. (2012) The proteomics of lipid droplets: structure, dynamics, and functions of organelle conserved from bacteria to humans. J. Lipid. Res. 53: 1245-1253

Yang, Z., Niu, Y., Ma, Y., Xue, J., Zhang, M., Yang, W., et al. (2013) Molecular and cellular mechanisms of neutral lipid accumulation in diatom following nitrogen deprivation. Biotechnol. for biofuels 6:67

Yoneda, K., Yoshida, M., Suzuki, I., Watanabe, M. M. (2016) Identification of a major lipid droplet protein in a marine diatom *Phaeodactylum tricornutum*. Plant Cell Physiol. 57: 397-406.

Zaslavskaia, L. A., Lippmeier, J. C., Kroth, P. G., Grossman, A. R., Apt, K. E. (2000) Transformation of the diatom *Phaeodactylum tricornutum* (Bacillariophyceae) with a variety of selectable marker and reporter genes. J. Phycol. 36: 379-386.

TABLES

Table 1. List of the proteins identified from the lipid droplet fraction.

Gel fraction	Mascot score			Sequence coverage [%]			Protein ID	Protein name	Functional domain (amino acid region)	Amino acid number	mol wt [kDa]	NCBI reference no	Similar protein in *Thalassiosira pseudonana*
	R1	R2	R3	R1	R2	R3							
4	1113	378	190	43	41	34	Phatr48859	Stramenopile-type Lipid Droplet Protein, StLDP	none	456	48.774	XP_002183367	hypothetical protein [XP_002292405]
5	50	45	41	13	5	9	Phatr48778	acyl-CoA binding protein	Acyl-CoA binding region (14-96)	351	38.195	XP_002183443	acyl-CoA binding protein, partial [XP_002289611]
2	60	-	-	33	-	-	Phatr54019	heat shock protein, Hsp70	HspA1-2,6-8 like nucleotide-binding domain (7-382)	653	70.831	XP_002177351	heat shock protein 70 [XP_002291508]
4	40	-	-	20	-	-	Phatr45894	hypothetical protein	Thioredoxin-like (171-260)	354	37.97	XP_002180271	hypothetical protein [XP_002286222]
1	-	-	37	-	-	5	Phatr49981	hypothetical protein	2OG-Fe(II) oxygenase superfamily (102-323), SAD/SRA domain (363-476)	544	60.786	XP_002184813	hypothetical protein [XP_002294418]

Table 2. List of the proteins identified in a previous report (Nojima et al. 2013) and its homologs in *P. tricornutum*.

ProteinID	**Putative function**	**mol wt [kDa]**	**Homolog in *Phaeodactylum***
g4796	transmembrane protein	85	Phatr44488/50592
g6705	ABC transporter, partial	149	-
g6574	potassium channel	58	Phatr13578
g4301	unknown, DOAP1	53	Phatr48876
g5708	unknown	49	Phatr45146

FIGURES

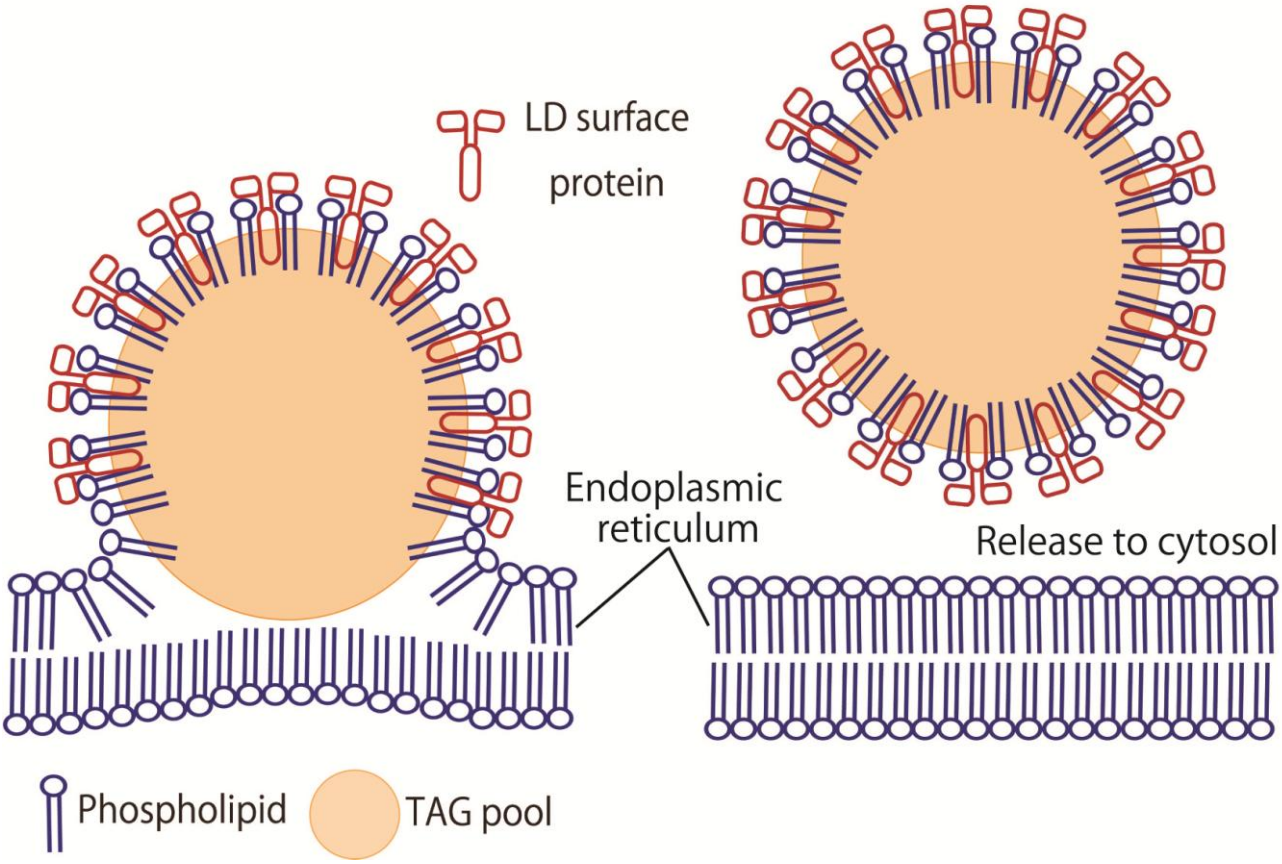

Figure 1. Basic model of lipid droplet formation.

Triacylglycerol (TAG) accumulates between the phospholipid leaflets of endoplasmic reticulum (ER). Size of lipid globule gradually increases and finally it was released into cytosol with specific surface protein.

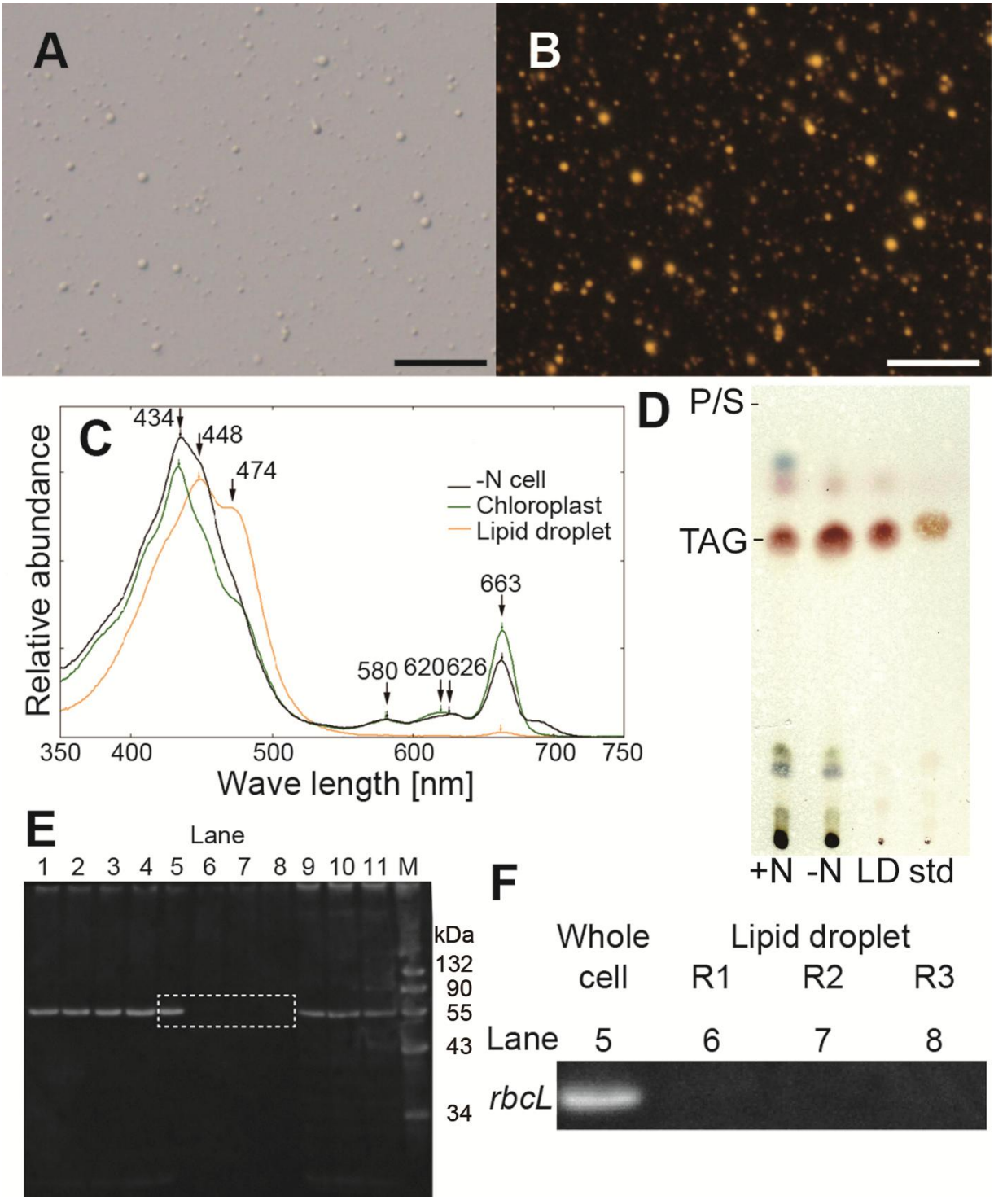

Figure 2. Quality evaluation of the isolated lipid droplet fraction.

(A, B) Microscopic image of a Nile-red stained lipid droplet. Scale bars indicate 20 μm. (A) Differential interference contrast image. (B) Fluorescence image. (C) Absorption spectra of acetone extracts obtained from nitrate (N) deprived whole cells (black line), chloroplast (green line), and lipid droplet (yellow line). (D) Silica-gel thin layer chromatography of lipid extracts obtained from whole cells (+N, nitrate sufficient; −N, nitrate deficient); lipid droplets from –N cells (LD); and triglycerol standard, triolein (std). P/S indicates peak of developing solvent. (E) Western blotting results against rbcL antibody. Lane 1–5: proteins from the whole cell. Lane 6–8: proteins from the lipid droplet fraction (replicate 1–3, respectively). Lane 9–11: proteins from the whole cell extract washed with acetone in the same manner as the lipid droplet fraction. M indicates the marker lane. (F) Magnified image of the white dotted area in E. R1–3 indicates samples from the three biological replicates.

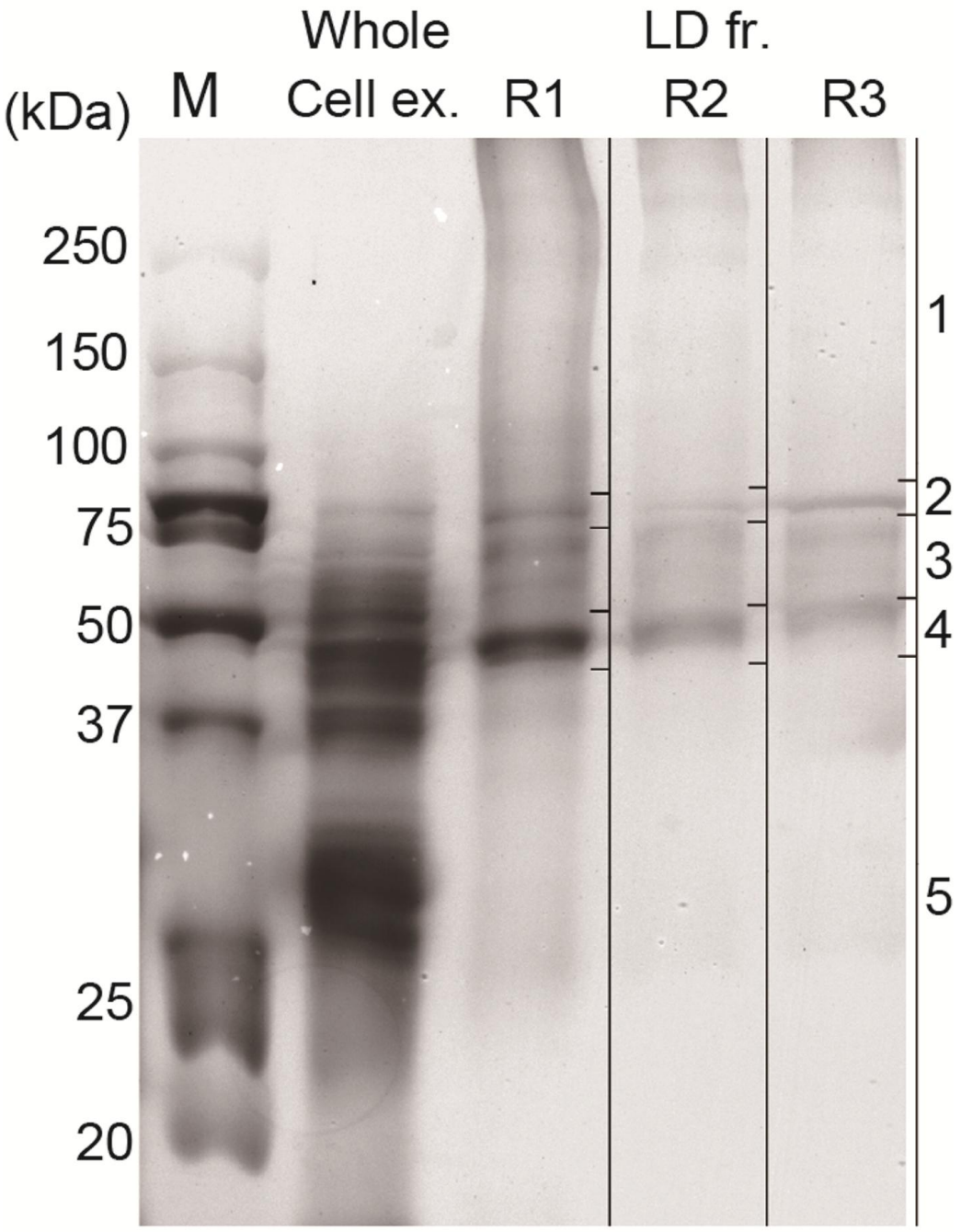

Figure 3. SDS-PAGE gel image of proteins from the whole cell extract and the lipid droplet fraction.

All lanes of the lipid droplet fraction (R1–3) were sliced into numbered gel pieces for proteomic analysis, as indicated at the right side.

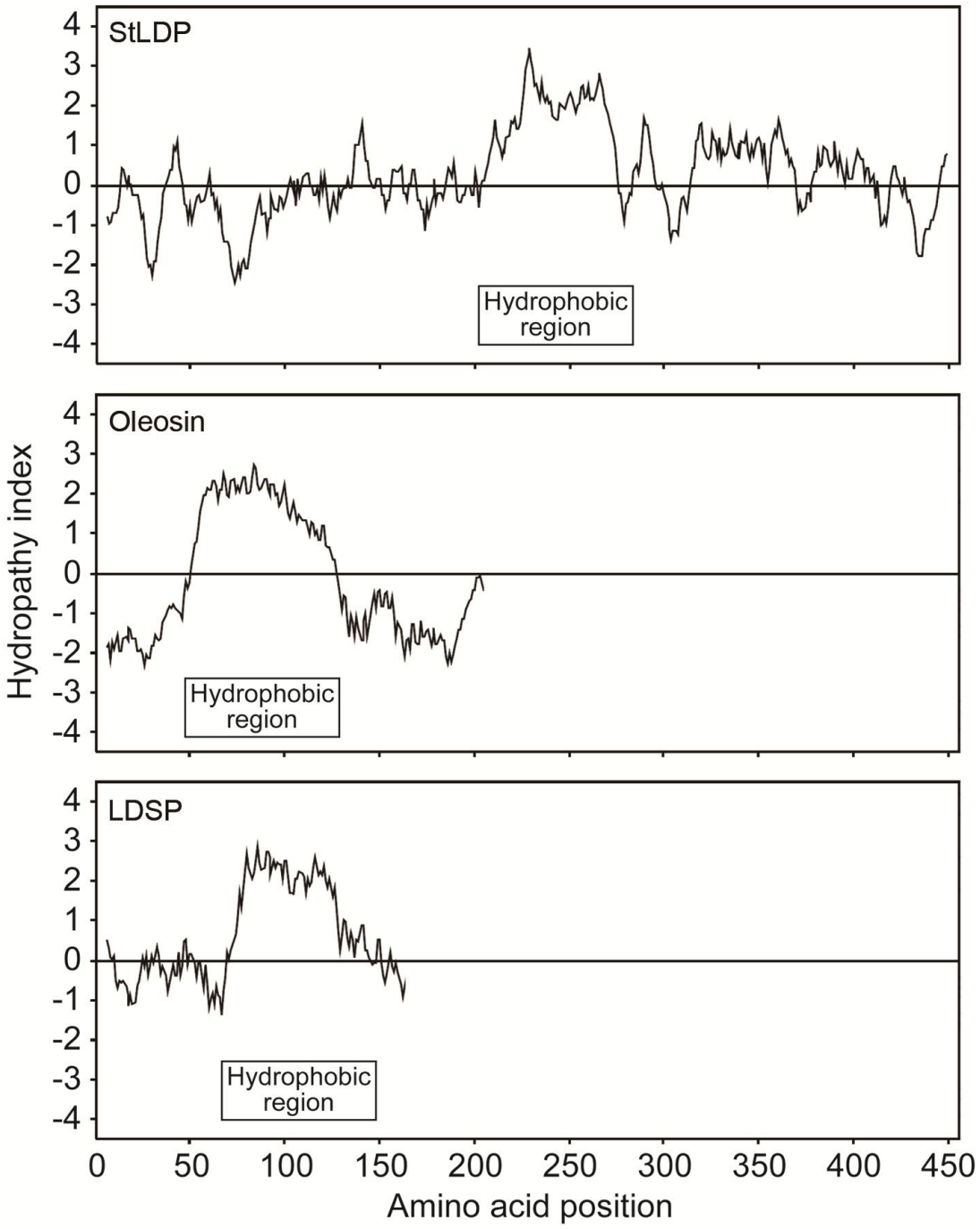

Figure 4. Hydropathy plots of StLDP, oleosin, and LDSP. For this analysis I used an amino acid sequence of StLDP (*Phaeodactylum tricornutum*, NCBI accession no. XP_002183367), Oleosin (*Arabidopsis thaliana*, GenBank: AAA87295), and LDSP (*Nannochloropsis* sp. CCMP1779, GenBank: AFB75402).

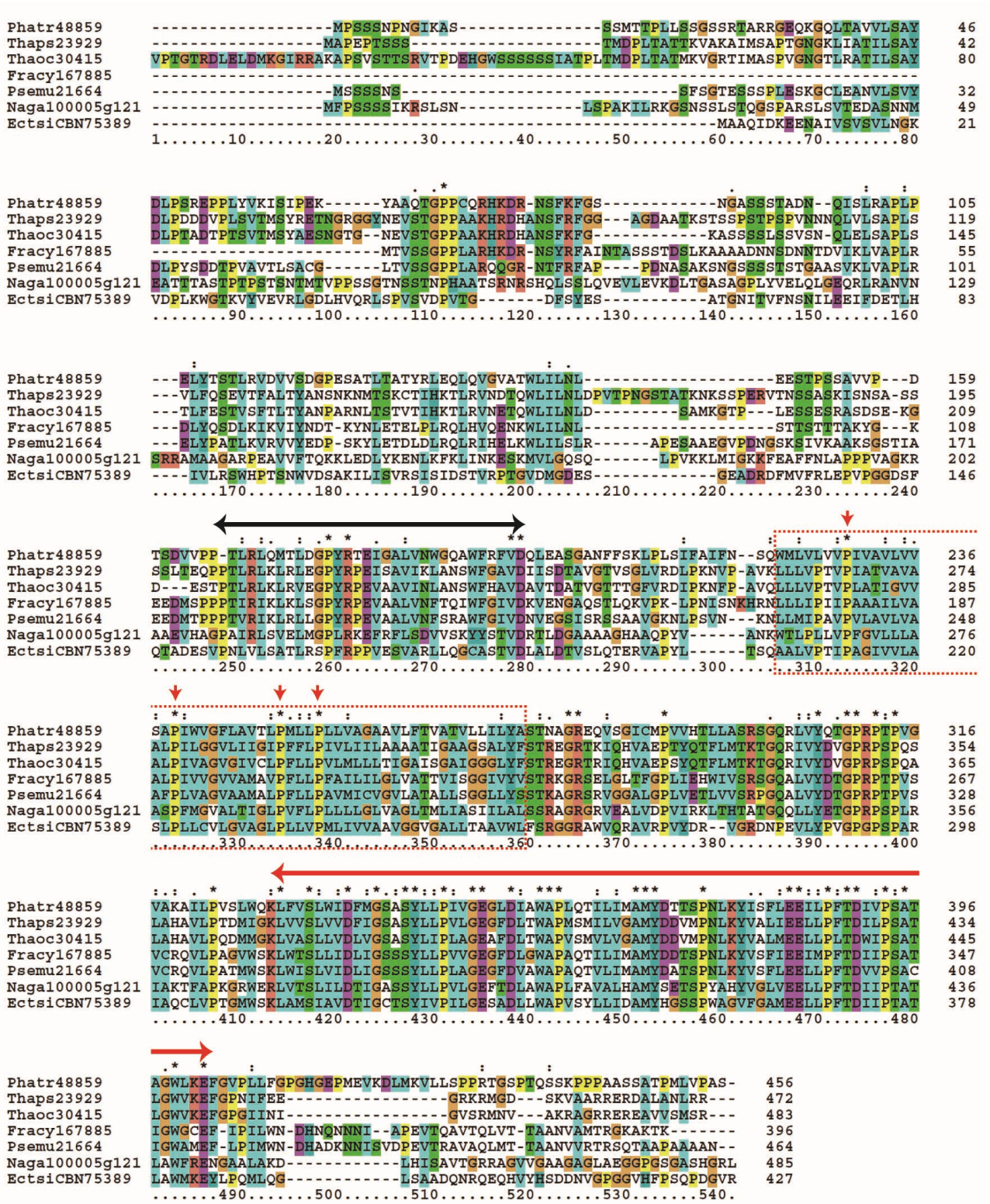

Figure 5. Multiple sequence alignment of StLDP and homologs.

The red dotted square indicates the hydrophobic domain conserved in the StLDP homologs. Small red arrows indicate the conservative proline residue in the hydrophobic region. The black two-headed arrow indicates a short conserved domain in the N-terminal side and the red two-headed arrow indicates a widely conserved domain in the C-terminal side. Fracyl167885 (*Fragilariopsis cylindrus*, JGI protein ID: 167885), Psemu21664 (*Pseudo-nitzschia multiseries*, JGI protein ID: 21664), Phatr48859 (*Phaeodactylum tricornutum*, JGI protein ID: 48859), Thaps23929 (*Thalassiosira pseudonana*, JGI protein ID: 23929), Thaoc30415 (*T. oceanica*, JGI protein ID: 30415), Naga100005g121 (*Nannochloropsis gaditana*, GenBank: EWM25464), and EctsiCBN75389 (*Ectocarpus siliculosus*, GenBank: CBN75389).

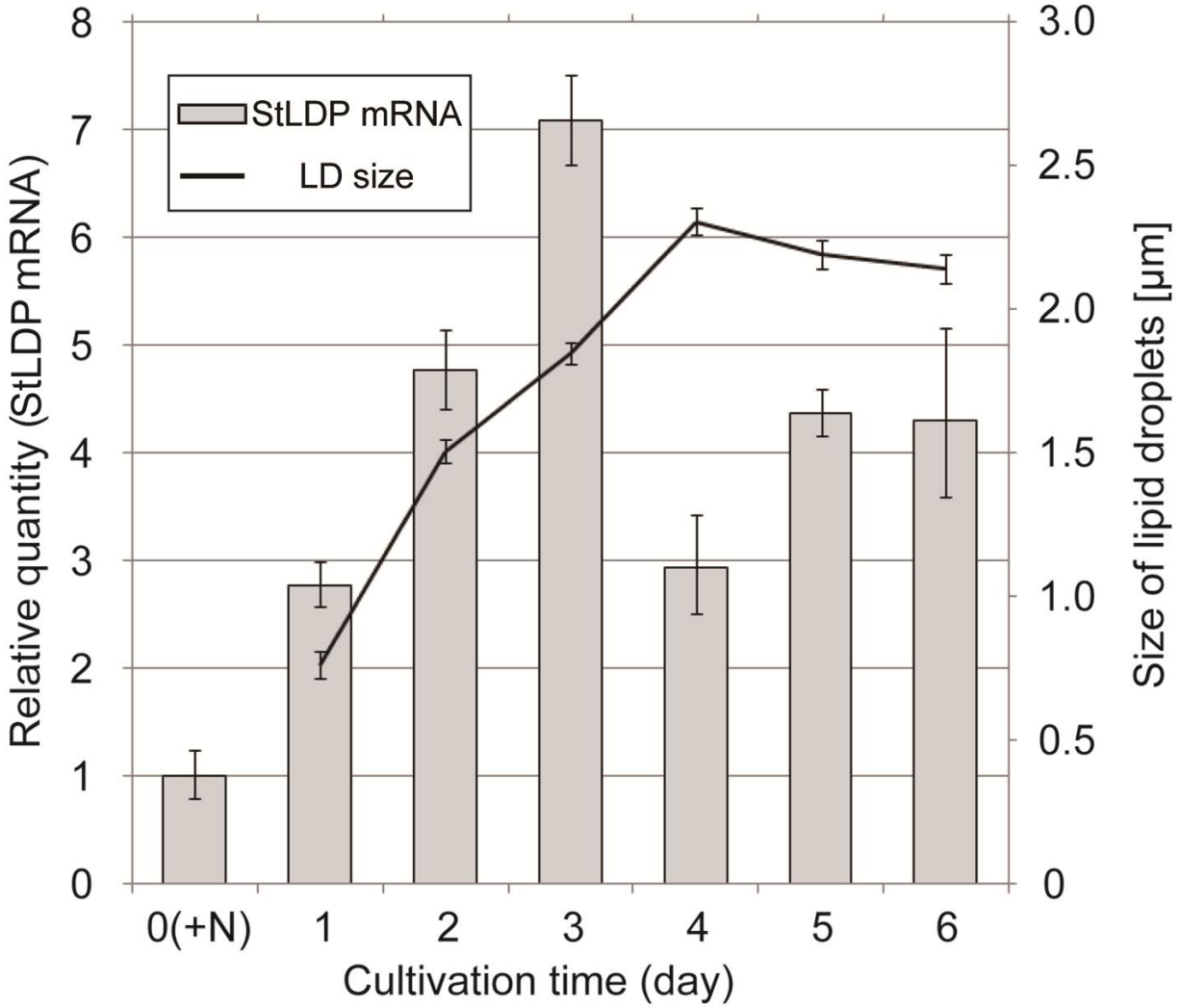

Figure 6. Changes in StLDP mRNA expression level and lipid droplet diameter during nitrate deprivation. Expression level was normalized using the housekeeping gene actin12 and the comparative C_t method; the error bars indicate S.D. (n = 3). Lipid droplet diameters were determined using the Nile-red stained cell image and the scale bars indicate S.E. values (n > 80).

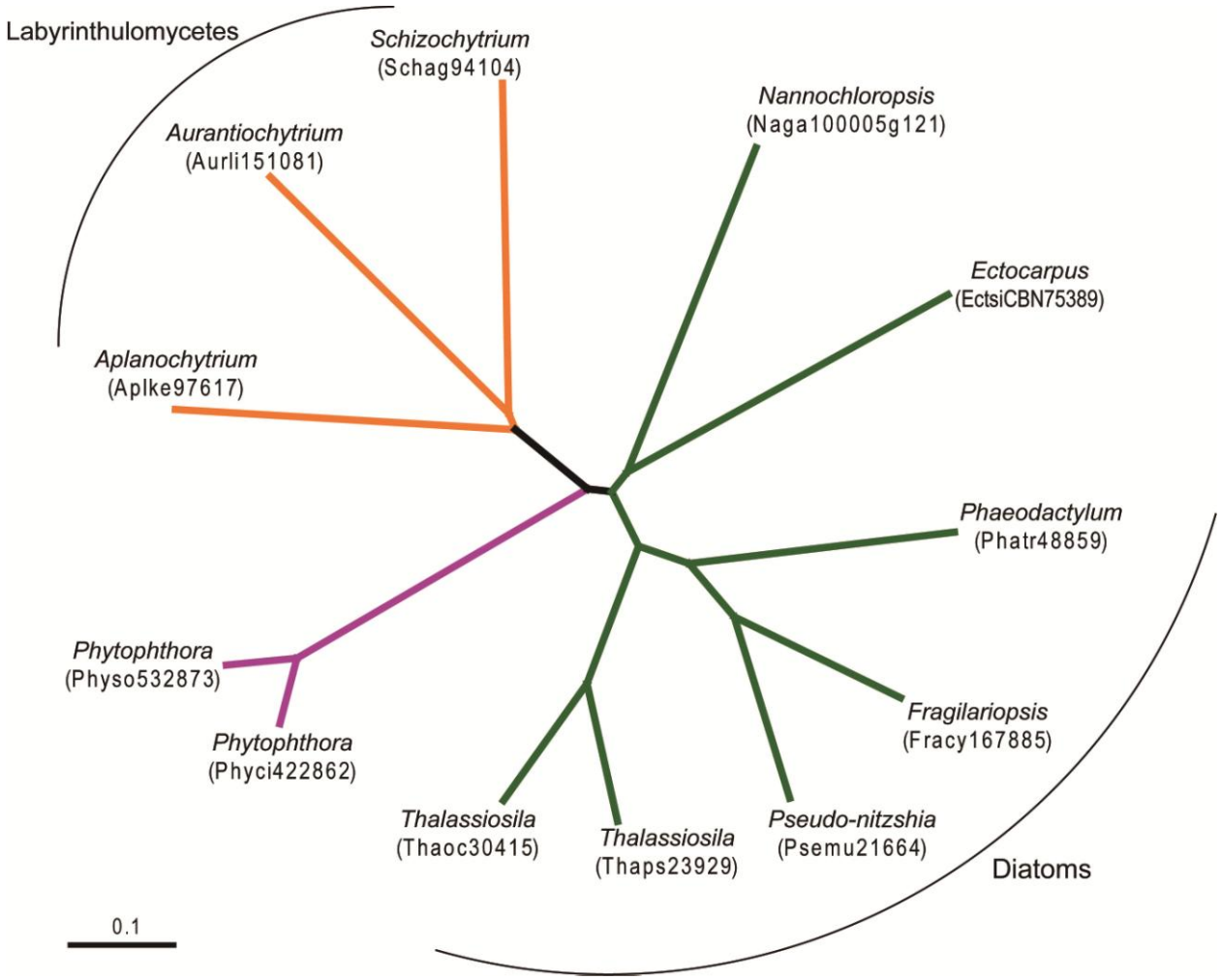

Figure 7. Unrooted phylogenic tree of StLDP orthologs in the Stramenopiles.

Green lines indicate Heterokontphyta, yellow lines indicate Labyrinthulomycetes, and purple lines indicate *Phytophthora* group. The amino acid sequences were used for phylogenic analysis with neighbor-joining method. The sequences used are the same as those described elsewhere.

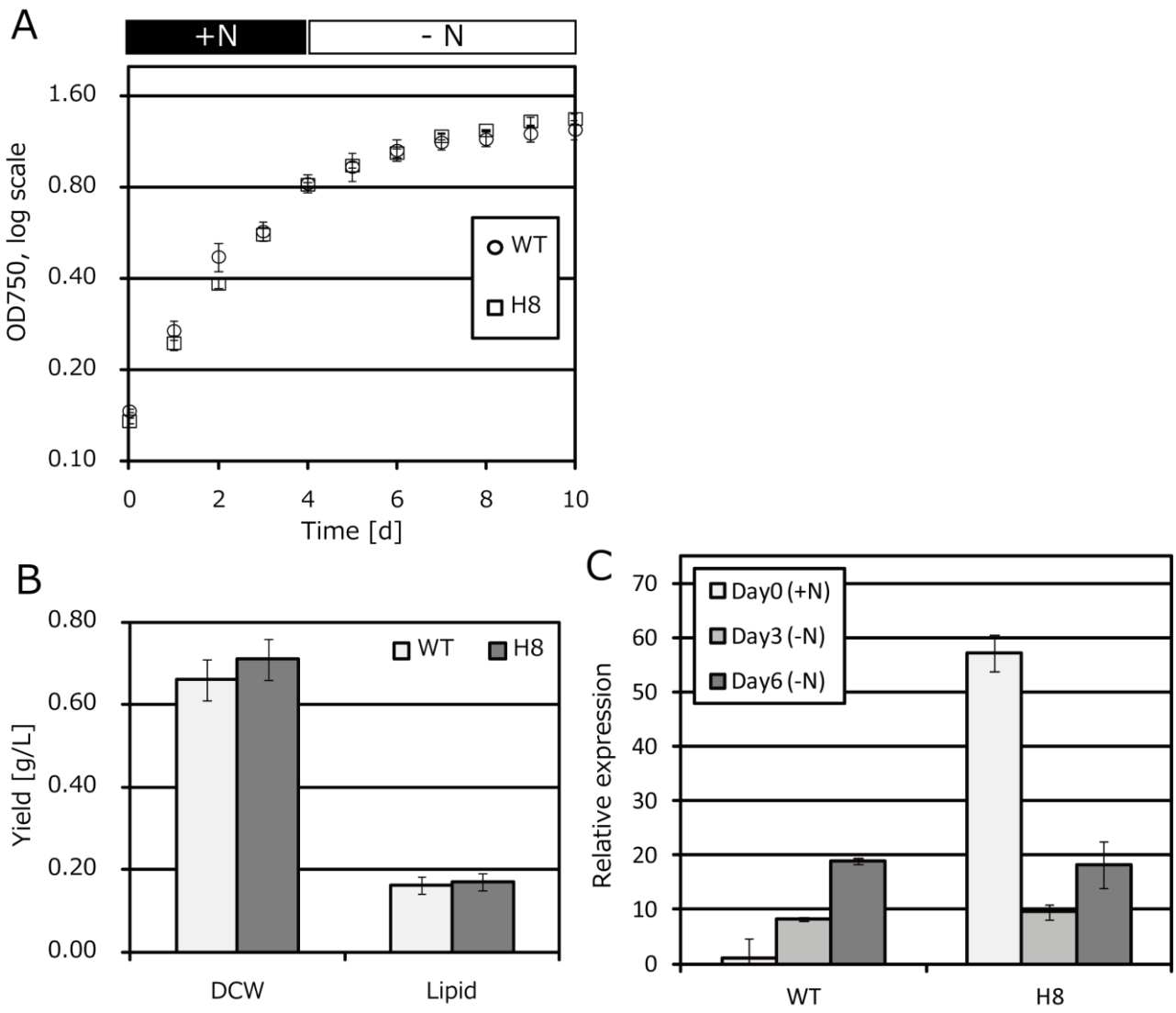

Figure 8. Growth curve, dry cell weight (DCW) and crude lipid amount, expression level of StLDP.

(A). Growth curve of wild type (WT) and StLDP-expressing mutant (H8). The cells were cultivated in nitrogen sufficient medium for 4 days then in nitrogen lack medium for 6 days. Open circles indicates WT and open squares indicates H8. Values as mean OD_{750} ± SD (n = 3).

(B). DCW and crude lipid amount at the end of cultivation in WT and H8. (C). Relative expression of StLDP measured by Realtime qRT-PCR. The expression level was measured with the sample at the initial day on re-inoculation into nitrogen lack medium (+N, Day 0), 3-days, and 6-days cultivated in nitrogen lack medium (-N, Day 3, Day 6, respectively). The expression on WT at Day 0 was regarded as one and relative expression level was drawn in the figure. Error bars indicates SD (n = 3). Actin12 was used as housekeeping gene for normalization.

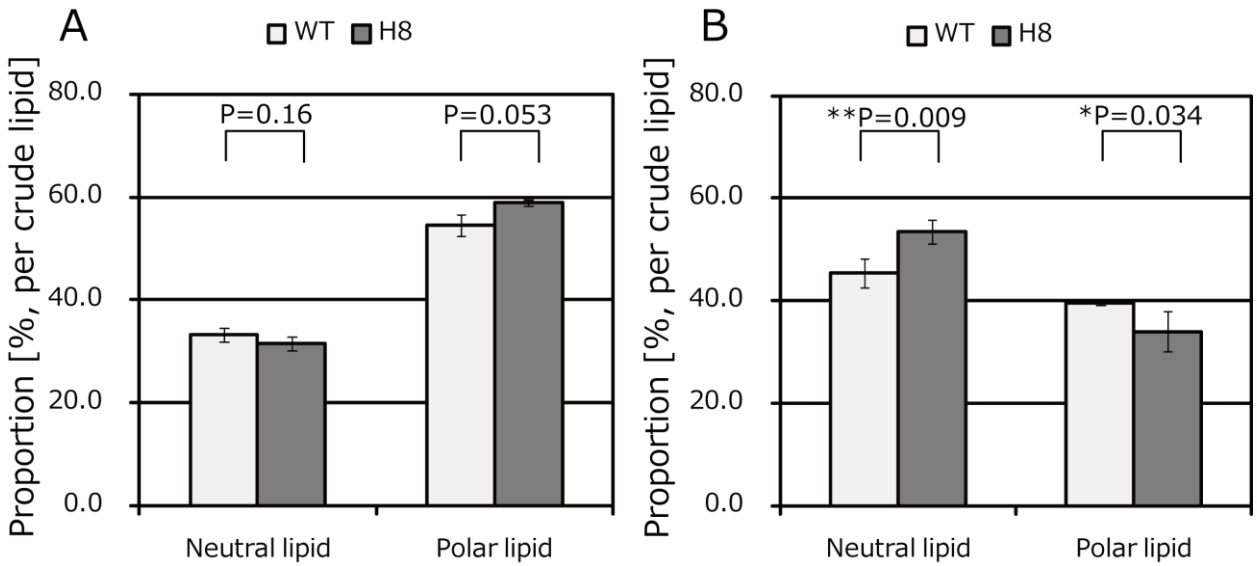

Figure 9. Proportion of neutral and polar lipid in crude lipid extract of WT and H8 mutant.

Neutral lipid and polar lipid composition in WT and H8 at Day 0 (A) and at Day 6 (B).

Error bars indicate SD value and statistical analyses were performed with Student's t-test (*P < 0.05, **P < 0.01, n = 3, one-tailed).

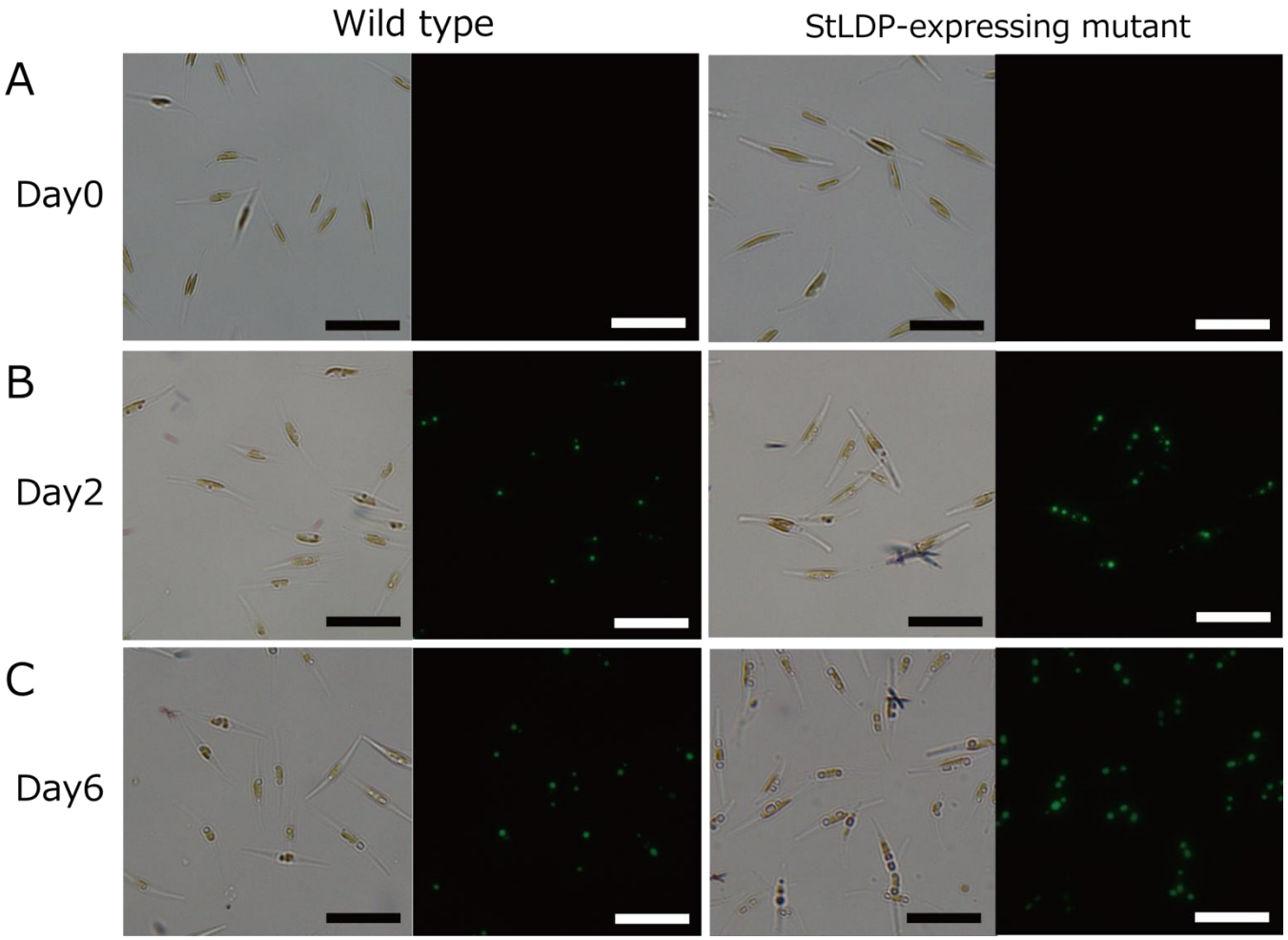

Figure 10. Microscopic images on lipid droplet formation in WT and H8 mutant.

Nile red staining cells at Day 0 (A), at Day 2 (B), and at Day 6 (C). Fluorescent images were captured through BNA green filter. Lipid droplets containing neutral lipid stained green with the BNA filter. Scale bars indicate 10 μm.

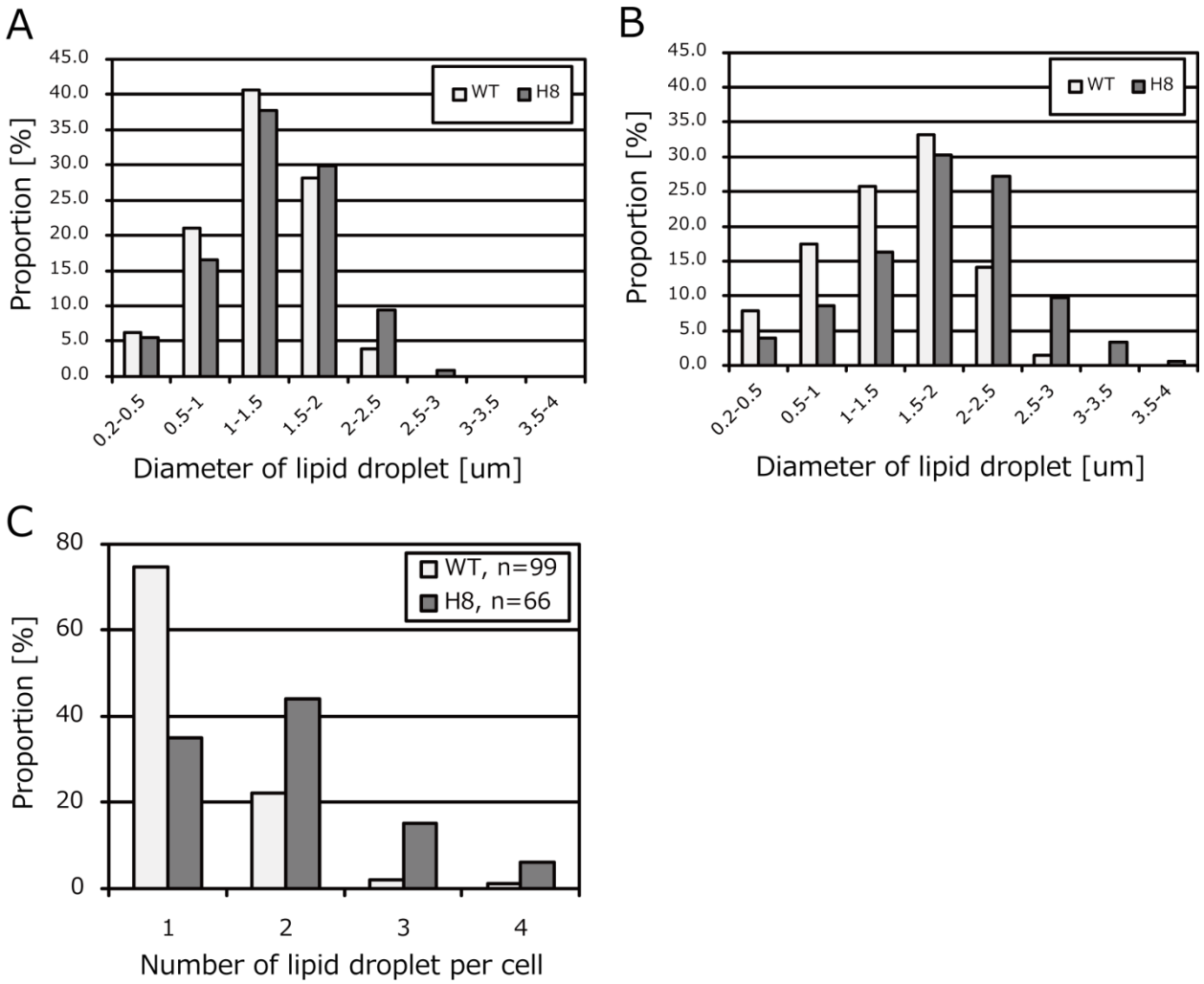

Figure 11. Distribution of diameter of respective lipid droplets and the number of lipid droplet in single cell.

Size distribution of lipid droplet at Day 2 (A) (WT: n = 128, H8: n = 151) and at Day 6 (B) (WT: n = 268, H8: n = 350). Each droplet size was measured using ImageJ. The number of lipid droplets per cell at Day 2 (C) (WT: n = 99, H8: n = 66).

SUPPLEMENTARY INFORMATION

Table S1. Composition of the modified Mann and Myers medium

Compound	
$NaNO_3$	50 mg
K_2HPO_4	5 mg
Na_2SiO_3 $9H_2O$	30 mg
Vitamin B_{12}	0.05 µg
Biotin	0.05 µg
Thiamine HCl	10 µg
NaCl	1.5 g
$MgSO_4$ $7H_2O$	360 mg
KCl	180 mg
$CaCl_2$ $2H_2O$	120 mg
Na_2EDTA $2H_2O$	30 mg
H_3BO_3	6 mg
$FeSO_4$ $7H_2O$	2 mg
$MnCl_2$ $4H_2O$	1.4 mg
$ZnSO_4$ $7H_2O$	33 µg
$Co(NO_3)_2$ $6H_2O$	7 µg
$CuSO_4$ $6H_2O$	2 µg
Tris (hydroxymethyl) aminomethane	100 mg
pH was adjusted with HCl at 8.0	
Distilled water	100 mL

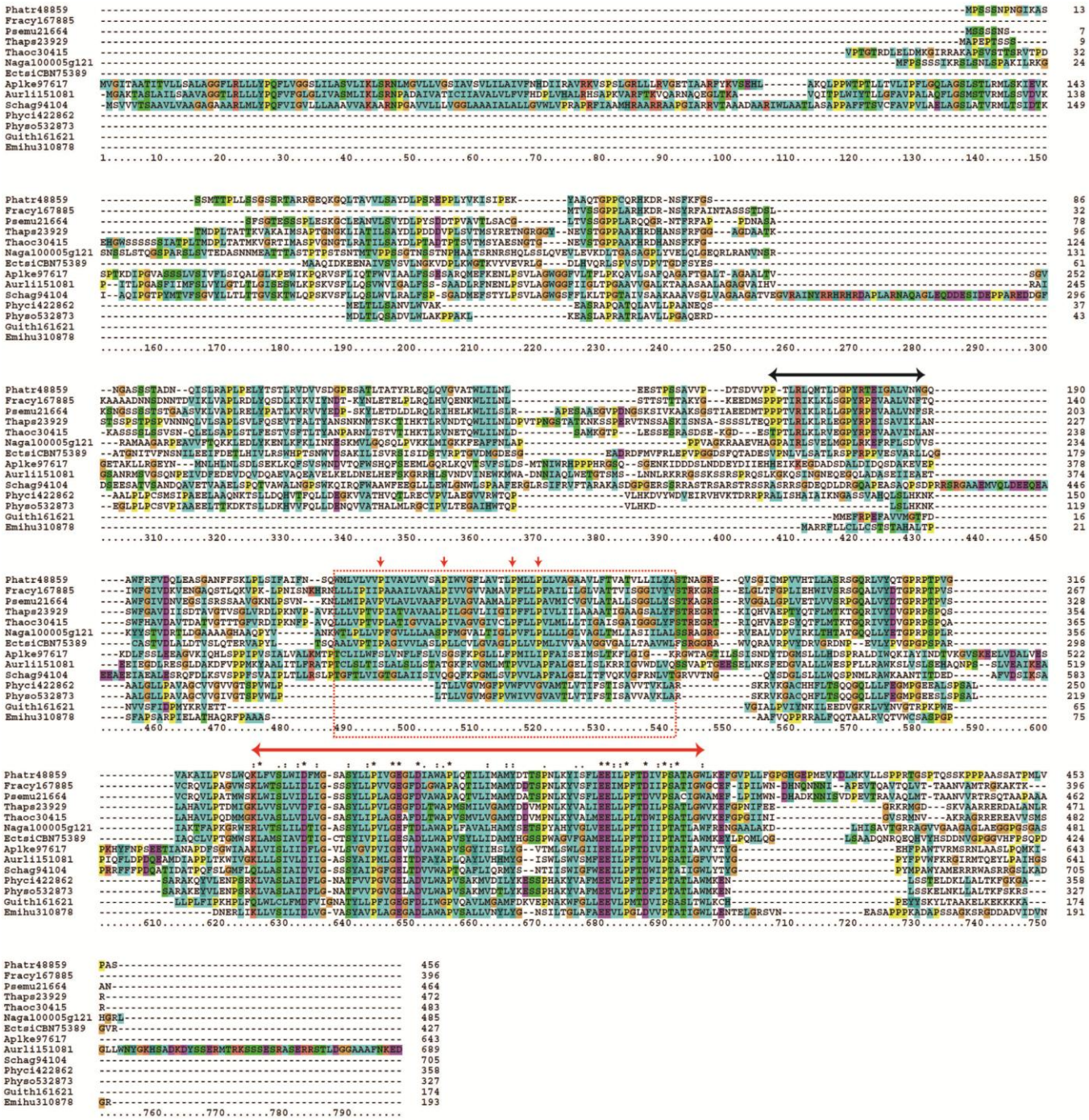

Figure S1. Multiple sequence alignment of StLDP orthologs.

The red dotted square indicates the hydrophobic domain in the StLDP homologs. Small red arrows indicate conservative proline residues in the hydrophobic region. The black two-headed arrow indicates a short conserved domain in the N-terminal side and the red two-headed arrow indicates a widely conserved domain in the C-terminal side.

Amino acid sequences used in this analysis are as follows; Phatr48859 (*Phaeodactylum tricornutum*,JGI ID: 48859), Fracyl167885 (*Fragilariopsis cylindrus*, JGI ID: 167885), Psemu21664 (*Pseudo-nitzschia multiseries*, JGI ID: 21664), Thaps23929 (*Thalassiosira pseudonana*, JGI ID: 23929), Thaoc30415 (*Thalassiosira oceanica*, JGI ID: 30415), Naga100005g121 (*Nannochloropsis gaditana*, GenBank: EWM25464), EctsiCBN75389 (*Ectocarpus siliculosus*, GenBank: CBN75389), Aplke97617 (*Aplanochytrium kerguelense*, JGI ID: 97617), Aurli151081 (*Aurantiochytrium limacinum*, JGI ID: 151081), Schag94104 (*Schizochytrium aggregatum*, JGI ID: 94104), Phyci422862 (*Phytophthora cinnamomi*, JGI ID: 422862), Physo532873 (*Phytophthora sojae*, JGI ID: 532873), Guith161621 (*Guillardia theta*, JGI ID: 161621), and Emihu310878 (*Emiliania huxleyi*, JGI ID: 310878).